Title
Structures and Materials in Stretchable Electroluminescent Devices

Journal
Advanced Materials, 34(22)

ISSN
0935-9648

Authors
Yin, Hexing
Zhu, Yuan
Youssef, Kareem
et al.

Publication Date
2022-06-01

DOI
10.1002/adma.202106184

Peer reviewed

Structures and Materials in Stretchable Electroluminescent Devices.

*Hexing Yin,[1] Yuan Zhu,[1] Kareem Youssef,[1] Zhibin Yu,[2] Qibing Pei [1]**

[1]Soft Materials Research Laboratory
Department of Materials Science and Engineering
Henry Samueli School of Engineering and Applied Science
University of California
Los Angeles, CA 90015, USA
E-mail: qpei@seas.ucla.edu

[2] Department of Industrial and Manufacturing Engineering, High-Performance Materials Institute, FAMU-FSU College of Engineering, Florida State University, Tallahassee, FL 32310

Abstract:

Stretchable electroluminescent (EL) devices have been obtained by partitioning a large emission area into areas specifically for stretching and light-emission (island-bridge structure). Buckled and textile structures have also been shown effective to combine the conventional light emitting diode fabrication with elastic substrates for structure-enabled stretchable EL devices. Meanwhile, intrinsically stretchable EL devices which are characterized with uniform stretchability down to microscopic scale are relatively less developed but promise simpler device structure and higher impact resistance. The challenges in fabricating intrinsically stretchable EL devices with high and robust performance are in many facets, including stretchable conductors, emissive materials, and compatible processes. For the stretchable transparent electrode, ionically conductive gel, conductive polymer coating, and conductor network in surface of elastomer have all been proven useful. The stretchable EL materials are currently limited to conjugated polymers, conjugated polymers with surfactants and ionic conductors added to boost stretchability, and phosphor particles embedded in elastomer matrices. These emissive materials operate under different mechanisms, require different

electrode materials and fabrication processes, and the corresponding EL devices face distinctive challenges. This review aims to provide a basic understanding of the materials meeting both the mechanical and electronic requirements and important techniques to fabricate the stretchable EL devices.

Keywords: stretchable electronics, electroluminescent device, stretchable emissive material, stretchable transparent electrode.

1. Introduction

The field of stretchable electronics has seen accelerating growth since the first report of wrinkled thin metal films on elastomer substrates in 1998 [1]. Stretchable circuits[2], thin film transistors (TFTs)[3], sensors[4], actuators[5], batteries[6], displays[7], and their hybrid systems[8] have inspired numerous applications.[9] Multiple stretchable electronic elements could be integrated as an "electronic skin" and conformably attached on skin, where ~30% surface strain needs to be tolerated.[10] It is also desirable to weave electronic functions into textiles without sacrificing wearing comfort. In many scenarios, the stretchable electronics need to visually deliver bio signals or electric outputs to users under twisted, crumped, elongated, or dynamically moving conditions. These demand a stretchable display, a core element of integrated human-machine interaction systems. Stretchable displays could also stimulate new concepts of collapsible and portable devices, such as rollable smartphones and television curtains.

Today, most wearable electronic devices on the market, such as smart watches and wrist bands, still feature a rigid screen. While Apple Watches use flexible organic light-emitting diode (OLED) displays, the screen is not stretchable. Even though the screen on the watches is non-deformable, the bendability of the OLED display unit enables a more compact assembly than a display unit based on glass could. A stretchable display would dramatically expand the benefits in both packaging and user experiences. Comparing to flexible display, the "expandable" characteristic of stretchable display allows it to only consume little space during storage and transportation. Thanks to its high tolerance to tensile strength, stretchable display might be stretched to appropriate size and be conformally attached on desired surface. Owing to its outstanding mechanical compliance and resilience, after usage stretchable display might be released from the surface and naturally shrink back to original shape. However, the development of stretchable displays is still at an early stage. One major challenge has been to develop a stretchable light emission technology which is scalable to the size of display screens, can be pixelated to high resolution, is thin, and can be integrated with an active-matrix driver, in addition to meeting the requirements of deformability, brightness, and efficiency.

Light-emitting or EL devices play a key role in flat panels for high-resolution information displays, from smart phones to television sets. Inorganic LEDs (ILEDs) are generally used as the backlight source for liquid crystal displays (LCDs).[11] Displays based on OLEDs as the directly emitting pixels are rapidly growing thanks to their high color gamut and wide viewing angles. OLEDs, as well as quantum dot LEDs (QLEDs), have enabled curved, foldable, and flexible displays. Micro-LEDs (μLEDs) are also emerging for the next generation displays.[12]

To a lesser degree, light-emitting electrochemical cells (LECs) and alternating current electroluminescent (ACEL) devices have been under development owing to their simple device architectures and facile fabrication methods that are compatible with large-area printing, and polymer substrates. For the time being, LECs and ACELs are arguably the best options for developing stretchable displays. Although all these EL devices have distinct working mechanisms, they share a common feature in terms of device structures that usually consist of one or multiple thin layers sandwiched between two electrodes. This feature allows the introduction of flexibility which generally increases with decreasing thickness. Flexible EL devices can be realized when the overall structure is ultrathin (a few microns or less) or constitutional materials are soft. Gustafsson et al.[13] demonstrated the first flexible OLED in 1992, where thin layers of polyaniline (PANI) on polyethylene terephthalate (PET) and poly[2-methoxy-5-(2-ethylhexyloxy)-1,4-phenylenevinylene] (MEH-PPV) were used as the anode and emissive layer, respectively. The cathode was calcium (Ca), which was <100 nm thick. Flexible EL devices have since received extensive developments, both in academia and industry.[14] The most exciting outcome is perhaps the foldable phones and tablet computers introduced to the market by Samsung Electronics and several other companies.

Stretchability, on the other hand, is much more challenging to obtain than flexibility or bendability. The stretchable EL devices must be capable of enduring repeated and reversible elongation and relaxation at large strains, which cannot be achieved by merely reducing the thickness of an intrinsically unstretchable device. To fabricate stretchable EL devices, firstly, an appropriate elastomer substrate must be selected to provide mechanical compliance and

resilience (complete shape recovery after large elongation). Secondly, the electronic performance of the devices must be preserved after repeated stretch and release cycles. In certain applications, the change of electronic characteristics of the devices at the maximum deformation also needs to be minimized. To realize stretchable EL device, two general design approaches have often been taken. One is interconnecting unstretchable EL units via stretchable geometries or architectures. The performance of the individual EL units is maintained as the elastic structures deform to undertake the external stretching while the EL units experience little tensile strain. These are categorized as structure-enabled stretchable EL devices. The other approach is fabricating stretchable EL devices only using stretchable materials. The devices prepared via this approach are classified as material-enabled stretchable EL devices, which are also called intrinsically stretchable EL devices. Comparing these two categories, the structure-enabled stretchable EL devices generally exhibit more robust EL performance, while the material-enabled ones are mechanically more robust.

Figure 1 illustrates the evolution of stretchable EL devices since 2009 when Rogers et al.[7] reported a stretchable ILED array. The number of publications has skyrocketed since then pursuing new materials and architectures.[15] For structure-enabled stretchable EL devices, transitions of research focus depended on the development of novel elastic structures, like from initial island-bridge structures to buckling structures and more recently to textile structures. For material-enabled stretchable EL devices, developing the essential stretchable materials and simplifying fabrication procedure moves the needle.

In this review, we survey the recent publications in the field of stretchable EL devices and discuss the critical challenges in the corresponding materials and architectures. We elaborate how stretchability is introduced to each type of stretchable EL devices and discuss the rationales behind the material selection and device fabrication process. The working mechanisms of the organic/polymer LEDs, LECs, and ACEL devices are first briefly described as a prelude to the subsequent discussions on stretchability. Then, three important stretchable structures: island-bridge structure, buckling structure, and textile structure applied in structure-enabled stretchable EL devices are discussed with related materials and fabrication issues. Next, relevant to material-enabled stretchable EL devices, three categories of intrinsically stretchable transparent electrodes are described, including ionically conductive gels, conducting polymer coating on elastomer substrate, and percolation network of conductive 1-D materials embedded in elastomer surface. Stretchable emissive materials will then be examined. These include conjugated polymers that could be directly stretchable in the OLED architecture, conjugated polymers made stretchable by the addition of surfactants or ionic conductors, and ZnS phosphors dispersed in elastomers in the ACEL devices. This review aims to provide a basic understanding in the materials selection and process development for future stretchable EL displays.

2. Electroluminescent devices and their stretching compatibility:

To date, various EL devices including ILED, OLED, QLED, LEC and ACEL devices have been investigated as EL units for stretchable display. These devices have distinct working mechanisms and put forward a higher request to materials and structures, which further limits

the introduction of stretchability. Thus, to introduce and optimize stretchability, it is necessary to firstly discuss their principle. In this section, electroluminescence mechanisms of ILED, OLED, QLED, LEC, ACEL devices are briefly introduced along with their adaptability to stretching.

2.1 ILEDs

Electroluminescent light emission is widely obtained in III-V semiconductors like gallium arsenide (GaAs), gallium phosphide (GaP), and indium gallium nitride (InGaN). The ILEDs based on these materials are fabricated through successive depositions via molecular-beam epitaxy or plasma-enhanced chemical vapor deposition on sapphire or silicon. To fabricate stretchable LEDs using such brittle ILEDs, Rogers et al.[7] developed an exfoliation technique to "peel off" the function layers of 2.5 μm thickness from the silicon substrate. The resulting ILEDs have certain bending flexibility and may be connected by strain-accommodating interconnects on stretchable substrates.[16] Meanwhile, thin film EL devices such as OLEDs and QLEDs are inherently more flexible, and more readily re-engineered to obtain intrinsic stretchability.

2.2 OLEDs

OLEDs share similar thin-film layered structure as the ILEDs, but their emissive layers are made of organic conjugated small molecules or light-emitting polymers (LEPs) (**Figure 2**a). The OLEDs that employ LEPs as EL layer are also referred to as polymer OLEDs or PLEDs. The energy barrier at the electrode/EL layer interface is a critical issue affecting the charge

injection efficiency. Overall, holes must overcome the energy barrier between anode and the highest occupied molecular orbital (HOMO) of the organic EL material, while electrons must overcome the barrier between the cathode and the lowest unoccupied molecular orbital (LUMO), as shown in **Figure 2**b. Often, a hole injection (HIL) layer and electron injection layer (EIL) have to be inserted at the anode and cathode interfaces to facilitate charge injections. The electron-hole recombination forms excitons with finite binding energy and lifetime. The decay time constant is on the order of a few nano seconds for the singlets and a few microseconds for triplets. To prevent quenching of the excitons on the electrodes or the HIL and EIL layers, hole transporting layers (HTLs) and electron transporting layers (ETLs) are often added to confine the excitons. The HTL and ETL layers also help mitigate the interfacial energy barrier via a stepwise energy level cascade (**Figure 2b**).

Small molecule OLEDs are commonly deposited in vacuum through physical vapor deposition, while PLEDs are fabricated through solution processes. Another important difference between these OLEDs is that, because polymers are mechanically more resilient than small molecules, PLEDs appear to be a more promising candidate for intrinsically stretchable EL devices.

2.3 QLEDs

QLEDs have similar working mechanism and device structure as OLEDs, except that quantum dots (QDs) are employed as the EL material. Core-shell QDs have been developed with a high photoluminescent quantum yield (PLQY) and a narrow emission spectrum, ideal for high color gamut pixels. Such QDs are nowadays widely used on QLED TV screens to improve the image

quality of LCD panels. The QLEDs-based EL devices in this review emit light when electrons and holes recombine within the QDs.[17] The core of the QDs are semiconducting nanocrystals of cadmium selenide (CdSe), lead selenide (PbSe), indium phosphide (InP), perovskites, and mixed compounds. Their diameters are typically in the range of 2 to 10 nm, where the quantum confinement not only provides a means to vary the optical bandgap but also leads to narrow emission spectra. A layer of QDs would not be stretchable. To introduce stretchability, one may disperse QDs in a polymer matrix as color conversion layers in stretchable EL devices.[18] Alternatively, QLEDs have also been fabricated first on a flat substrate and subsequently transferred onto a pre-stretched elastomer substrate.[19] The periodic wrinkles formed in the QLED layer after elastomer relaxation allow for reversible stretching. These will be further discussed in the buckling structure section.

2.4 LECs:

LEC was introduced initially to eliminate the charge injection barriers in OLEDs and thus simplify the device architecture.[20] As illustrated in **Figure 2**c, a typical LEC consists of an EL layer sandwiched between two electrodes. The EL layer contains both the EL material, which is also the electronic (semi)conductor, and an ionic conductor (or solid electrolyte).[21] The mixed conductor layer undergoes electrochemical doping when a bias above E_g/e is applied (**Figure 2**d). The n-doping of the semiconductor on the cathode facilitates electron injection whereas p-doping at the anode facilitates hole injection. Doped conjugated LEPs are highly conductive, as such the EL layer could be made much thicker than 100 nm without incurring substantial increase in driving voltage. On the other hand, the formation of the p-i-n junction

is a dynamic process; a number of factors could affect the kinetics of the junction formation, including thickness and ionic conductivity. Also, the junction disappears after the bias is removed. Other mechanisms may also play a role, such as the accumulation of cations on the cathode surface and anions on the anode surface at $V < E_g/e$.[22] The electrodynamics may also affect the charge injections, though the junction formation is desired for high brightness and device efficiency.

Several features of the LECs make them promising candidates for intrinsically stretchable EL devices. First, the device structure can be as simple as a sandwich of a single emissive layer between two electrodes. This makes it easier to match the mechanical properties at the interfaces to sustain deformations and minimize delamination and crack formation. Second, the removal of the charge injection barriers indicates that there is no need to match the electrode work function with the LUMO or HOMO of the emissive material. Therefore, there is more freedom to choose stretchable and transparent electrode materials. Last but not the least, relatively thick emissive layer can be used, which makes the emissive layer easier to deposit and more tolerable to defects and thickness non-uniformity.

2.5 ACEL devices:

ACEL devices discussed in this review refer to the light-emitting devices operating under a hot-electron impact excitation mechanism. (**Figure 2**f) A high electric field applied across a dielectric layer generate the hot electrons. Luminescent phosphor particles embedded in the dielectric absorbs the kinetic energy of the electrons and generate visible photons. The ACEL devices are usually operated at high voltages, such that a modestly conductive electrode can

distribute current over large areas. The dielectric layer or layers may be fairly thick, > 50 μm, to keep the leakage current low, though larger thickness leads to higher operating voltages. Thus, an electrode/phosphor powders-dielectric EL composite/electrode structure is formed for basic ACEL devices (**Figure 2**e). ZnS phosphor particles developed for fluorescent lighting are commonly used as the EL materials thanks to their availability and high luminescent efficiency. The dielectric are usually elastomers such as silicone and acrylate. Dielectric of high permittivity is desired because it can concentrate the applied field on the ZnS phosphors and enhance device performance. On the other hand, if the phosphors are surrounded by dielectric of low dielectric constant, potential drop will mainly occur within the matrix.[23] The following equation elucidates the relationship between applied field on phosphors and dielectric constant of matrix:[24]

$$E_{ZnS} = E_m \left[\frac{3\varepsilon_{r2}}{2\varepsilon_{r2}+\varepsilon_{r1}-f(\varepsilon_{r1}-\varepsilon_{r2})}\right] \quad (1)$$

where $E_m = V/d$, V is the applied voltage and d is the thickness of phosphor powders-dielectric EL composite. f is the volume fraction of ZnS phosphors. ε_{r1} and ε_{r2} are the dielectric constant of spherical grain of ZnS grains and polymer matrix, respectively. High ε_{r2} can increase E_{ZnS}. The relationship between brightness and applied voltage of ZnS phosphors ACEL device can be expressed in the following equation:[24]

$$L = L_0 \exp\left(\frac{-b}{\sqrt{V}}\right) \quad (2)$$

where L represent brightness, V is the applied voltage. L_0 and b are constants related to the dielectric constant of the dielectrics, and dimension of the phosphor particles. Generally, an electric field E_m > 5 V/μm and operation frequency > 1k Hz are required for stretchable ACEL devices to achieve brightness > 100 cd/m^2. High operating bias and frequency are the main obstacles for ACEL devices to be used as wearable EL devices.[25]

3. Critical materials and processing for structure-enabled stretchable EL devices

Stretchable EL devices based on intrinsically un-stretchable EL units may be considered being comprised of three key elements: the brittle EL units, an elastomer substrate, and stretchable structures. They have very mismatched moduli. To improve overall stretchability, architectures have been designed to isolate tensile strain off the EL units during stretching while allowing large deformation.[7, 26] The most successful strategies developed so far to integrate the three key elements are island-bridge structures, buckling structures, and textile structures. Table 1 summarizes the representative structure-enabled stretchable EL devices, their key elements, and device performance.

3.1 Island-bridge structure

The island-bridge structures consist of rigid EL units, the "island" and highly stretchable interconnects, the "bridge", and an elastomer substrate. The interconnects are structured like a weaved net, with the EL units at the nodes, and are assembled on the elastomer surface, embedded in-plane[27] or buckled out-of-plane[26b], depending on specific applications. During stretching, the interconnects take majority of strain and extend remarkably, while EL units only

experience little strain (usually < 1%). The relationship between stretchability of the interconnects and entire system could be expressed as:[28]

$$\varepsilon_{system} = \left(1 - \sqrt{f}\right)\varepsilon_{int} \quad (3)$$

where ε_{system} and ε_{int} represent stretchability of the system and interconnects, respectively. f is the filling ratio defined as the ratio between islands-covered area and overall area of system. This equation indicates a trade-off between overall stretchability and filling ratio, and the limited stretchability that interconnects can contribute to system. For example, for stretchable display with roughly equal area of interconnects and EL units (f = 0.5), the stretchability of system is only 0.29 times of that of the interconnects. Thus, to have decent overall stretchability without sacrificing filling ratio, ε_{int} must be large. In most cases, the interconnects are made of thin metal films of serpentine or wavy structures[29], stretchable conductive composites[26a, 30], or serpentine photoresist coated with metal.[31] A general fabrication process to pattern the metal interconnects involves photolithography, e-beam deposition and lift-off steps. The interconnects as well as the LEDs are transfer-printed on elastomer surface.[29, 32]

Strain management in the island-bridge structure is challenging. There is a steep strain variation at the deformable-rigid interfaces as the rigid EL units constrain the elastomer under them from expanding during stretching. The large strain variation could cause delamination of the EL units from the elastomer substrate. The interface between the EL units and the interconnects may also detach due to localized strain under stretching.

To suppress localized strain at these rigid-soft interfaces, thin layers of a stiff material such as SU-8 photoresist[33] or polyimide[34] could be added within the elastomer as a platform to form "strain-insulated islands". This architecture requires the thickness of the platform to be much smaller than that of the substrate. In addition, the following inequation should be met:[35]

$$E_{platform} \cdot t_{platform} \gg E_{substrate} \cdot t_{substrate} \quad (4)$$

where E and t represent equivalent elastic modulus and thickness. For instance, Robinson et al.[36] embedded two polyimide pieces within polydimethylsiloxane (PDMS) substrate (**Figure 3**a). One small piece was placed near the surface of PDMS, and the other large piece was buried at around half of the thickness of the substrate. The finite element analysis (FEA) result (**Figure 3**b) indicated that these two films formed a dual-disk structure which suppressed surface strain and achieved a smooth strain transition at the island-bridge interface. In another work by Drack et al.[37], stretchable LED stripes were demonstrated with out-of-plane wrinkle interconnections. To fabricate the structure, thin metal films of copper (or gold) were firstly evaporated onto a 1.4-μm-thick PET foils with shadow mask to define the geometry. Polyimide thin film coupons (2 mm*2 mm*0.05 mm) were sandwiched between two 3M™ VHB™ films, which was used as the elastomer substrate (**Figure 3**c). Metal interconnects along with the ultrathin PET film were then transferred onto the pre-stretched elastomer substrate to induce buckling. White light-emitting LEDs were placed on the elastomer at where the polyimide coupons were embedded. The Cu winkles interconnects and the whole LED stripe could be uniaxially

stretched up to 275% and 240% strain, respectively. Twisted at 720°, the LED stripe could be stretched to 140% (**Figure 3**d). When the interconnects in both x axis and y axis were applied, the resultant LEDs networks achieved biaxially strain in an area expansion ratio of 2.5 without device performance degradation.

Recently, adding stretchable stress-relief structures or thin layers under rigid EL units has been shown to enhance the stretchability of OLED based island-bridge structures. For instance, Lim et al.[31] inserted arrays of PDMS pillars between PDMS substrate (Young's modulus 1.5 MPa, Poisson's ratio 0.49) and SU-8 layer (Young's modulus 4.2 GPa, Poisson's ratio 0.22). SU-8 served as both substrates for OLEDs and zigzag interconnects. During stretching, the SU-8 interconnects extended along with the PDMS substrate, so did the section of the pillars in contact with the substrate. However, the other section of the pillars which was in contact with SU-8 rigid islands maintain their spacing so that the stress would not be applied on the islands (**Figure 3**e and **3**f).[31] Comparing devices without and with the PDMS pillars array, the peak stress of the interconnects decreased from 70 MPa to 58 MPa, and that of the islands from 6.38 MPa to 4.35 MPa. Owing to compact zigzag interconnect design and effective stress management, The OLED array had up to 44% filling ratio (sum of the emissive area over the entire surface area at un-stretched state) and 35.3% elongation (**Figure 3**g). The turn-on voltage was 4 V, maximum luminance was 1000 cd/m^2 at 6.7 V, and the maximum current efficiency was 3 cd/A at peak brightness. The luminance at a constant 6.5 V decreased by 19% after 1000 repeated stretch-release cycles between 0 and 20% strain. Kim et al.[38] took a different approach for stress relief where a thick ultrasoft silicone elastomer layer (Silbione; Young's

Modulus ~ 0.9 kPa) was inserted in between PDMS substrate and SU-8 layer (**Figure 3**h). Their experiment results showed that the maximum stretchability of the interconnects was increased from 170% to 350% as the modulus of Silbione was decreased from > 10 kPa to 0.9 ± 0.02 kPa. The resultant OLED arrays could be stretched up to 40% strain corresponding to the 140% maximum stretchability of the interconnects (**Figure 3**i). At 0.9 kPa modulus, this Silbione layer is somewhat like a paste, the OLED coupons could be removed by smearing.

Island-bridge structures have been the most broadly explored architecture for stretchable EL devices. The high EL performance at fairly large strains has been obtained by a number of groups. Meanwhile, there are also disadvantages that warrant further attention. One inherent problem of the island-bridge structures is that the interconnects take up in most cases more than 50% of the surface area.[39] The serpentines and winkles often have comparable or larger scale than the EL units, indicative of an aperture ratio of less than 25%. During stretching, the elongation of the interconnects further reduces the aperture ratio. Low aperture ratio usually leads to low brightness and low resolution. Thus, hyperelastic interconnects of small area fractions are desired.[40] Another issue for out-of-plane interconnects is that these fragile, choppy three-dimensional (3D) structures are difficult to be used in displays where front panels are sealed with flat glass. Encapsulation could also be complicated.[41] Some planar serpentine interconnects deform out of plane when elongated, which causes similar package problems as the out-of-plane structures.

3.2 Buckling structure

Unlike islands-bridge structures where EL units are largely in plane with the interconnects, the buckling structure stacks thin active EL layers on the relief surface of the elastomer substrate. Stretchable EL devices of buckling structures are usually fabricated by first depositing the active EL layers on an ultrathin film substrate. Then, the EL layers and the ultrathin film are transferred together onto a pre-stretched elastomer substrate. When the pre-strain is released, the stiff but bendable thin layers are subjected to the compressive strain from the elastomer substrate and deform perpendicular to the stress direction, forming periodic wrinkle structures. During stretching, these winkles gradually flatten until the elastomer substrate expands to about the pre-strain level. Commonly used ultrathin films include commercially available PET[42] and polyimide[19] thin sheets. OLEDs[43] and QLEDs[44] are the main device types used in the buckling structures thanks to small thickness and flexibility of the EL layers.

The buckling pattern formed from a thin stiff layer and soft elastomer substrate may be estimated by [45]

$$\lambda = 2\pi h_f \left[\frac{(1-{v_s}^2)E_f}{3(1-{v_f}^2)E_s}\right]^{1/3} \quad (5)$$

where λ is the wavelength of buckling period, h_f is the thickness of stiff layer. v_s and v_f are the Poisson ratio of substrate and ultrathin film, respectively. E_s and E_f are the Young's Modulus of substrate and ultrathin film, respectively. This equation predicts the linear relationship between the wavelength of wrinkles and the thickness of the stiff layer. Achieving wrinkles of small wavelength is of great importance for stretchable displays. Macroscopic EL wrinkles

(wavelength of a few hundred microns) can distort pixels and are perceptible to naked eyes as "wavy" image. As such, the flexible EL layers and their substrate should be as thin as possible. For OLEDs and QLEDs, the active EL layers are well below 1 μm thick. The buckling pattern is mainly determined by the ultrathin substrate. Reducing the thickness of the EL substrate also alleviates the surface strain of bended EL devices, as shown in **Figure 4**a. The surface strain of a bilayer structure is [46]

$$\varepsilon = \left(\frac{t_f+t_s}{2r}\right)\left[\frac{1+2\eta+\chi\eta^2}{(1+\eta)(1+\chi\eta)}\right] \quad (6)$$

where $\eta = t_f/t_s$ and $\chi = E_f/E_s$. r is the bending radius. t_f and t_s are the thickness of thin film and substrate, respectively. E_f and E_s are the Young's moduli. According to this equation, the thinner the film, the less surface strain EL devices need to endure. In other word, under the critical surface strain that leads to device failure, thinner films allow smaller bending radius.[15c] This is because at certain bending radius, neutral planes of thinner polymer substrates are closer to the surface where devices are located. In practice, the ultrathin film substrate should be less than 2 μm thick.

For example, Kim et al.[47] reported QLED fabricated on a 1.7-μm-thick polyethylene naphthalate (PEN) film. The QLED layers and the PEN substrate were transferred onto pre-strained (70% strain) PDMS. After releasing the pre-strain to form the surface wrinkles, a thin layer of Ecoflex was coated over the buckled QLED surface to encapsulate the QLED layers. The buckling wavelength was 185 μm, with a peak-to-valley amplitude of 53 μm and bending

radius of 35 μm (**Figure 4**b). Red, green, and blue lights were all fabricated in a similar fashion except for the use of particle size of the CdSe/CdS/ZnS and CdSe/ZnS QDs (**Figure 4**c). The red light-emitting QLED showed a maximum brightness of 1310 cd/m^2 and peak current efficiency of 2.25 cd/A. It could be stretched for 100 cycles between 0 and 70% strains with only a 12.3 % reduction in brightness. Li et al.[19] took a different approach and fabricated buckled perovskite QLEDs (**Figure 4**d). They used a polyimide thin film (2 μm thick) with silver nanowires (AgNWs) embedded in the surface as both the substrate and anode. The methylammonium lead tribromide ($MAPbBr_3$) QD layer and most other layers, except for the cathode, were solution processed on the anode. The ultrathin QLED was transferred onto a pre-stretched VHB elastomer substrate to form periodic wrinkles. The buckled AgNWs/polyimide on the VHB had a peak-to-peak distance of 100 μm and bending radius of 70 μm (**Figure 4**e). The QLEDs could be turned on at 3.2 V, with a peak current efficiency of 9.2 cd/A and peak brightness of 3187 cd/m^2. **Figure 4**f and **4**g show the device stretched up to 50% strain. This device could be stretched repeatedly by 20% strain for 1000 cycles, and its brightness decreased by 25%.

The formation of the wrinkle pattern could also be controlled by compartmentalizing the adhesion between the transferred thin film and elastomer substrate. The compartmentalization is usually achieved by creating periodic structures on the substrate surface.[48] For instance, Yin et al.[49] applied laser ablation on a VHB film and created periodic grooves (**Figure 4**h). When an OLED thin film was transferred and laminated on the grooved surface under pre-stretching in the lateral direction, it was adhered to the substrate only in the areas without laser ablation.

When the pre-strain was released, the OLED areas above the grooves buckled out-of-plane (**Figure 4**i). This approach allows to adjust the wavelength by forming grooves of different periods. They obtained a buckled OLED that could be stretched up to 100% strain (**Figure 4**j). In an alternative approach by the same group,[50] the surface grooves were formed by stretch fragmented silver coating on a VHB film (**Figure 4**k). To enhance the adhesion of laminated OLED film on the surface area without silver fragments, a roller with patterned protrusions was employed to press the thin film during the transfer. The OLED film areas pressed by the protrusions would stick to the VHB substrate. The adhesion period was thus in accord with the period of protrusions on the roller. The buckled OLED had a maximum stretchability of 100% (**Figure 4**l).

The buckling approach has two major issues. Firstly, handling the ultrathin EL film during the transfer process is tricky. The EL films are typically 1 to 2 μm thick and have a strong tendency to self-rolling or warping during peeling the films off the release substrate and attaching them onto the pre-stretched substrate. This problem escalates when the process is scaled up but may be resolved if the process is automated. Another problem is that the wrinkles are not perfectly periodic. After all, buckling occurs due to mechanical instability of the materials. When substrates are uniaxially pre-stretched, the resultant 1D winkles are still somehow predicable. However, if substrates were biaxially pre-stretched, the formed 2D wrinkles could be disordered due to anisotropic stress.[51] These wrinkles exhibit no pattern or period under stretch-release cycles. As a result, wrinkles of extreme small bending radius could form during the cycles and lead to device failure. This problem may be addressed according to a recent

report of directly depositing PLED on pre-stretched substrate to improve the predictability of the 2D wrinkles.[52]

3.3 Textile structure

Stretchable EL devices of textile structures have merged recently driving by the perception that wearable displays should be comfortable and breathable. Textiles are made of interlaced yarns or threads by weaving, knitting, braiding, etc. Small openings are left between adjacent fibers, allowing certain degree of stretchability along the diagonal direction. The stretchability can be enhanced by increasing the size of the openings or optimizing the weaving angles. There are three different approaches to exploit the stretchability of textile for stretchable EL devices: directly building EL devices on a textile substrate, forming EL elements at the interlaced nodes of woven fiber electrodes, and fabricating EL fibers and assembling them into textiles. Our discussions are focused on the first two approaches. Reader may refer to a recent review on EL fibers.[53]

EL devices fabricated directly on textile substrate may be considered intrinsically stretchable as each layer of the devices including the substrate is stretchable. As a matter of fact, textiles are not good substrates for solution-based EL devices due to their rough and porous surfaces. To date, ACEL devices have been mainly used for the textile substrates. For example, Zhang et al.[54] fabricated ACEL devices on spandex fabric. Their process started with depositing polypyrrole (PPy) on spandex fabric by the oxidative polymerization of pyrrole. PPy coating had a sheet resistance of 804 Ω/sq and roughness below 8 nm. A ZnS phosphors-silicone

emissive film and polyacrylamide (PAM) -LiCl hydrogel film were prepared separately on a release substrate. These films were then peeled off and attached on the PPy/spandex fabric. The resultant ACEL device exhibited a maximum brightness of 70 cd/m^2 when driving at 5 V/μm and 2k Hz. It could endure 100 cyclic stretching and releasing between 0 and 100% strain. Wu et al.[55] fabricated an ACEL device on ultrasheer fabric knitted with nylon and spandex fibers (**Figure 5**a). Gold was coated on the fabric via solution-based deposition. They showed that all fibers were covered by a layer of gold approximately 100 nm thick. The gold coated fabric had a sheet resistance of 3.6 ± 0.9 Ω/sq and transmittance of 37% at 550 nm wavelength. The transmittance further increased to 58% at 120% strain but then decreased to 47% at 200% strain due to area change of the openings. The global resistance of the fabric did not change more than 2 times up to 200 % strain. Two of the Au/fabric were used to sandwich a layer of ZnS:Cu-Ecoflex as the ACEL emissive layer. The device could be stretched up to 200%, twisted or conformed like a fabric (**Figure 5**b).

The second approach has been used for passive matrix displays where each EL unit is formed at the interlaced node between two intersected fiber electrodes. This method broadens the choices of materials and EL mechanisms because the roughness of the fiber electrode surface is controllable. However, the difficulty of fabrication lies on the exposed emissive coating which must withstand the assembly process such as weaving and knitting. In addition, stretching could be detrimental to the EL units due to localized friction at the nodes between two interlaced electrodes. One solution to solve these problems is to fabricate and encapsulate the EL units on the warp fibers and expose only electric contact for the weft fibers. In other

words, the weft is only used for conduction purpose, which leaves the EL units less vulnerable during stretching. For instance, Song et al.[56] demonstrated a wearable fibertronic OLED display (**Figure 5**c). Indium tin oxide (ITO) coated PET fibers (stripes of 2 mm width) were used as the anodes. Through a polyurethane (PU) mask, the OLED active layers and Al cathode were deposited on the anodes to define the pixel area. Meanwhile, Al was deposited on bare PET fibers as the conduction fiber. The OLED fibers and conduction fibers were orthogonally woven together. The resultant devices had a turn-on voltage of 2.3 V, peak luminesce of 4300 cd/m^2 at 5 V, and peak current efficiency of 46 cd/A. The woven OLED array could be stretched to 20% strain along the diagonal directions (**Figure 5**d). More recently, Shi et al.[57] prepared large-area display textiles based on co-woven PU ionic gel fibers (conductive wefts), nylon yarns coaxially coated with silver and ZnS:Cu-silicon (luminescent warps), and cotton yarns (**Figure 5**e). Both the PU ionic gel fibers and the ACEL/nylon yarns were coated with thin layers of silicone for protection. Large textile display of 6 m*25 cm were fabricated with approximately $5*10^5$ microscale ACEL devices formed between weft-warp interlace (**Figure 5**f). Each ACEL device exhibited brightness of 115.1 cd/m^2 when it was biased at 3.7 V/μm and 2k Hz. The display could be stretched along the diagonals for 1000 cycles, and the luminesce intensity of most EL units remained stable.

These stretchable EL devices of textile structures highlight the major advances in the field. Nevertheless, there is still much room for improvement. For the ACEL textiles, the high driving voltage and high frequency could be a major concern for wearable applications. Friction induced degradation, encapsulation that survives normal machine washing, and the integration

with active-matrix backplanes remain major challenges for the ACEL and other EL textiles. The holy grail is EL fibers woven into fabrics. Publications so far on EL fibers have focused on the fabrication of individual EL fibers.[58] These EL fibers usually exhibit lower EL performance than their planar counterparts in terms of brightness and luminesce efficiency, as it is difficult to deposit uniform EL materials on fiber surface.[59] There have been no systematic study on assembling EL fibers into fabrics and developing a suitable driving circuit for the assembly.

4. Critical materials and processing for material-enable stretchable EL devices

Without reliance on serpentine or winkle patterns, the essential architecture of an intrinsically stretchable EL device is simplified to a functional EL layer sandwiched between two electrodes. The payoff includes multifunctionality enabled by soft materials, easier processing, and competitively low costs.[60] The time between Yu et al.[61] demonstration of a stretchable polymer-LEC (PLEC) in 2011 to Zheng et al.[62] fabrication of high-density stretchable transistors has seen a tremendous growth in control over soft electronic materials processing. Nevertheless, required stretchability of each functional layer in an EL device reveals material limitations, namely EL performance. Another challenge is the balancing act of material modulus matching with optoelectronic performance in each layer to prevent interlayer delamination. Therefore, material development as well as proper integration into device fabrication process is key to realizing better and more scalable intrinsically stretchable EL devices. In this section, we review the development of stretchable materials for intrinsically stretchable EL devices in terms of electrodes and EL layers of LEDs, LECs, and ACEL devices.

4.1 Stretchable Electrodes:

Electrodes for EL devices usually refer to transparent conductive electrodes (TCEs). TCEs normally require high surface conductivity for efficient charge carrier injection, and high transmittance for light extraction. For EL devices with flat TCE sandwich structures, light can be emitted from both sides of the devices. If one-side-emission is expected, the other electrode should have high reflectivity of visible light so that reflected light escapes through the TCE. For rigid OLEDs, ITO is the TCE of choice. Metals like Al, Ag, and Ca are popular choices for reflective electrodes. Nevertheless, they are not stretchable in the form of thin film.[63] They do not function as electrodes in stretchable EL devices without additional treatment.[64] The development of stretchable electrodes on a suitable substrate is the starting point for intrinsically stretchable EL displays.

Different EL devices have specific electrode requirements mainly depending on the emission mechanism or intended application. For example, thin films in OLEDs and QLEDs are normally of tens to hundreds of nanometers.[65] As such, the surface roughness of the electrodes for those devices must be very small,[66] otherwise any protrusion in micron scale could easily poke through and short the device. The electrodes for ACEL devices, on the other hand, do not have strict roughness requirements. This is because the emissive layers of ACEL devices are usually tens of microns,[23] sometime even a few millimeters thick,[67] which offer much higher tolerance for electrode roughness. Although stretchability, transmittance, and conductivity are the main criterions to evaluate stretchable TCEs, other considerations on properties like self-

healing,[68] shape-memory,[61] and bio-compatibility[69] become viable when the TCE performance needed is more modest. The components of intrinsically stretchable electrodes are mostly 1) the conductive nanomaterials that provide a conducting medium, and 2) the elastomeric matrix that guarantees mechanical compliance. Based on the exact configuration, there are mainly three typical electrode structures (**Figure 6**): One, ionic conductors are uniformly dissolved in the entire elastomer matrix. Two, the conductive materials form a thin layer on the elastomer surface. Three, the conductive materials form a percolation network embedded into the surface of the elastomer matrix. Nowadays, a variety of conductive materials have been used in these structures, including metallic/carbon nanomaterials,[70] conducting polymers,[71] ionic conductors,[72] thin metal films,[73] etc. Polymers like silicone,[74] chitosan,[75] polyacrylamide hydrogels,[76] polyurethanes,[68] and poly(styrene-b-(ethylene/butylene)-b-styrene)[77] have been utilized as matrices of electrodes. In this section, these three typical structures as well as corresponding materials are discussed in detail. In Table 2 and Table 3, intrinsically stretchable TCEs and EL devices are summarized, respectively.

4.1.1 Ionically conductive transparent electrode

Ionically conductive gels including hydrogels have been under development for a variety of different applications.[67, 72, 76, 78] In recent years, these materials have also been investigated as the stretchable TCEs for intrinsically stretchable EL devices thanks to the optical transparency and mechanical toughness of certain ionically conductive gels.[57, 79] Stretchable transparent gel electrodes often use ionic liquids for the ionic conductivity.[79] In the case of hydrogels, salts are added as the ionic sources.[80] To prepare ionic liquid gel electrodes, an ionic liquid and

elastomer are co-dissolved in solvents and form a uniform solution (**Figure 6**a). The mixture is then coated on a substrate via drop-casting, spin-coating, or blade-coating to form the stretchable TCE. One can also cast the liquid solution into a mold to form electrodes of desired dimensions. In the case of hydrogels, monomers and oligomers of the target elastomer are used to harness both ionic and covalent bonding. In this case, a curing process is necessary to solidify the structure after solvent evaporation.[15b]

In the ionic gel TCEs, all components can be transparent to visible light, so the overall transmittance could be nearly 100%, minus light reflection at the surfaces. Ions are uniformly dissolved across the entire elastomer, so the conductivity is isotropic. The mobility of ions, in general, is much smaller than that of electrons. Ionically conductive electrodes typically have a conductivity $\sigma \sim 10^{-3}$ S/cm.[81] Thus, ionic conductive TCEs may not be suitable as the electrodes for ILEDs, OLEDs, and LECs which require high driving current densities. However, they can be used in ACEL devices which operate at high voltage but low current.

Ionic liquids of various kinds have been used, which tend to dissolve well in a range of polar elastomers.[82] Polymers containing hydrogen bond forming groups such as polyethylene glycol, chitosan, PAM, and mixtures thereof are used to form stretchable hydrogels.[83] The hydrogen bonds between the polymer chains and ionic-polar bonding between the ions and polymer chains can result in superior stretchability (> 1000% strain), while the ionic conductivity is hardly affected during stretching.[76]

In one report, Larson et al.[67a] admixed lithium chloride (LiCl) and PAM to fabricate a stretchable ion-conducting hydrogel. The LiCl water solution has high ionic conductivity (~10 S/m). LiCl also helps retain water within the hydrogel. PAM was employed as the elastomer matrix because of its high toughness and high transparency. The hydrogel electrode could be stretched up to 500% strain, with resistance increasing 2.5x when stretched to 400% strain. Stretchable ACEL devices, called light-emitting capacitors in this work, were demonstrated by sandwiching a ZnS-silicone composite between two hydrogel electrodes (**Figure 7**a). Maximum device stretchability up to 487% strain was achieved (**Figure 7**b). Meanwhile, Yang et al.[76] employed similar LiCl-PAM hydrogels in another ACEL device. Their hydrogels could be stretched over 20 times of its original length, with tensile strength below 60 kPa. The ACEL device showed remarkable stretchability up to 1500% strain and maximum brightness of 9.4 cd/m^2 driven at 3.6 kV and 1 kHz (**Figure 7**c). In another study by Zhang et al.,[78] stretchable hydrogels consisted of potassium hydroxide, poly(vinyl alcohol) (PVA) and PEO were prepared and utilized in fiber-shape ACEL devices (**Figure 7**d). In this special architecture, two parallel hydrogel electrodes of ellipse shape were co-extruded with the emissive layer through a needle (**Figure 7**e). The emissive layer consisted of ZnS powers and silicone. This PVA-PEO hydrogel was transparent (92% transmittance at wavelength 400 nm-850 nm) and could be stretched up to 800% strain (**Figure 7**f). The hydrogel showed ionic conductivity of 0.29 S/cm. Both the hydrogel and the fiber device could endure 1000 repeated stretch-release cycles up to 300% strain with little performance degradation. A maximum brightness of 233.4 cd/m^2 was achieved under 7.7 V/μm electric field and 2.5k Hz alternating bias frequency.

4.1.2 Transparent conductive thin layer coated on elastomer substrate

Conductive materials can be directly coated on the surface of an elastomer substrate via physical vapor deposition or solution process. (**Figure 6**b) To increase the film coverage and the wetting of the coating solutions, the elastomer is usually treated with UV/O_3 or oxygen plasma to introduce polar bonds on the surface.[71a] The conductive coatings are normally tens of nanometers thick or less; high transparency can be achieved through a combination of coating thickness and porosity. The elastomer serves as a substrate undertaking the applied stress and providing resilience during stretching. Nevertheless, the thin layer itself must be capable of maintaining its electrical continuity during stretching. For example, gold can be evaporated and form a thin layer on the surface of PDMS substrate. High transparency demands the thickness of gold thin layer to be less than 10 nm.[84] However, such thin layers cracked and disconnected at < 5% strain.[85] Conducting polymers and 1-D percolation network have proven to maintain conductivity under stretching and surpass uniform metal coatings. Poly(3,4-ethylenedioxythiophene):polystyrene sulfonate (PEDOT:PSS) is a widely used conducting polymer in flexible and stretchable electronics.[71b] Although pristine PEDOT:PSS thin film cannot endure strains greater than 5% due to its rigid nature, a very thin film can be doped with surfactants or be blended with elastomers to enhance the overall stretchability.[86] For instance, Lipomi et al.[87] introduced a PEDOT:PSS composition with 1 wt% of Zonyl fluorosurfactant (FS-300) and 5 vol% of dimethylsulfoxide. The blend solution was spin-coated on UV/O_3-treated PDMS substrates. A sheet resistance of 260 Ω/sq at 95% transparency was achieved with PEDOT:PSS thickness of 70 nm. The electrode can be stretched up to 188% strain. After 1000 cycles repeated stretch-release from 0 to 30% strain, the film resistance increased 400%.

PEDOT:PSS can also be blended with other polymers to enhance mechanical or electrical properties. In the work of Bade et al.,[88] PEDOT:PSS was mixed with high molecular weight PEO (average Mw ≈ 5,000,000) in aqueous solution, which was then spin-coated on a O_2 plasma treated PDMS substrate. A small percentage of PEO increased the conductivity of the thin film, which was explained by the configuration change of PEDOT chains from extended coil to linear.[89] A maximum conductivity of 35600 S/m was achieved when the PEO percentage was optimized at 33 wt% (**Figure 8**a). The resultant PEDOT:PSS-PEO/PDMS stretchable electrode achieved transmittance of 82% at 500 nm wavelength with sheet resistance of 140 Ω/sq. SEM images confirmed that no obvious morphology change after the electrode was stretched to 50% strain. Resistance increased by 12% when the electrode was stretched to 40% strain. The electrodes were then used in a perovskite-polymer LED, where $MAPbBr_3$-PEO blend was used as the emissive layer. The devices exhibited 2.4 V turn-on voltage, 15960 cd/m^2 maximum brightness at 8.5 V, 3.2 cd/A maximum current efficiency, and stretchability up to 40% strain (**Figure 8**b). The LEDs could be repeatedly stretched to 40% strain for 100 cycles.

Another common strategy to form stretchable conductive thin layers on an elastomer surface is to encapsulate it with another elastomeric material to form an interpenetrating conductor-polymer network film. The conductivity of the electrodes during stretch-release cycles is maintained because surrounding elastomer phase prevents the network from detaching or slipping and help dissipate mechanical energy. To fabricate this structure, one must minimize the disturbance on the conductive network when coating the precursor solution. In many cases,

the solution can swell the elastomer substrate below the conductive surface and destabilize the network. In addition, if the solution is spin-coated, high centrifugal force under spinning might also damage the network, especially when the solution is viscous or have large interaction with the conductive components of the network. Another challenge lies in the thickness control. For LEDs or LECs, the top surface of TCEs must be conductive. However, if the newly coated elastomer were too thick, it buries the otherwise exposed conductive surface. Most of the elastomers are insulators and can strongly hinder charge injection. Given these considerations, electrodes of such structures are mainly used in the ACEL devices where mild surface conductivity and rough thickness control are allowed as long as the electric field is high. For example, Wang et al.[90] spray-coated AgNWs/isopropanol on a PDMS surface to form a conductive network. Then, a mixture made of ZnS:Cu microparticles and PDMS precursor was spin-coated on top of the network (**Figure 8**c). Interestingly, although the liquid partially dissolved the PDMS substrate under the network, strong bonding was formed at the interface between newly coated PDMS and original PDMS substrate, which promoted the interaction between the emissive layer and the electrode. The resultant ACEL devices could be stretched up to 100% strain (**Figure 8**d) and survived after repeatedly stretch and release for 1000 cycles from 0 to 80% strain. The turn-on voltage was around 60 V, and the maximum brightness was nearly 40 cd/m^2 when the device was biased at ± 120V, 2.5k Hz. In another report, You et al.[91] applied a similar device structure with a different elastomer. In their work, polyurethane urea (PUU) was synthesized as the elastomer coating on AgNWs network. To evaluate the protecting ability of PDMS and PUU for AgNWs network, sandwiches of PDMS/AgNWs/PDMS and PDMS/AgNWs/PUU were prepared and tested via cyclic stretching and relaxation. For

PDMS/AgNWs/PDMS, obvious resistance fluctuation was observed during 5000 test cycles from 0 to 50% strain while PDMS/AgNWs/PUU exhibited uniform resistance variation during 5000 cycles of 0-100% strain (**Figure 8**e). It was suggested that the hydrogen bonding between the carbonyl groups of poly(vinylpyrrolidone) on AgNWs and carboxylic acid groups of PUU contribute to the stability. The resultant PDMS/AgNWs/PUU electrodes provided sheet resistant of 3 Ω/sq with transmittance of 70.1% at 550 nm wavelength. The electrodes were then used to fabricate ACEL devices, where ZnS phosphors-PUU was employed as the EL layer (**Figure 8**f). The device had hysteresis behavior during loading and unloading test, where approximately 6% residual strain could be found after stretched to 50% strain due to the viscoelasticity of PUU matrix. Both electrodes and the formed ACEL devices could be stretched up to 150% strain. A maximum brightness around 100 cd/m^2 was achieved when biased at 300 V and 500 Hz.

4.1.3 Transparent conductive network embedded in elastomer

Conductive materials can also form networks embedded in elastomers.[10, 61, 77, 92] Like the structure of conductive thin layers on elastomer surface, the optical and mechanical properties of embedded structure are dominated by the conductive networks and the matrix, respectively. In addition, embedding conductive network in an elastomeric substrate can significantly reduce surface roughness, which is critical for OLEDs.[93] In fact, most successful electrodes for stretchable OLEDs are of embedded structures. To prepare the composite electrode, conductive materials are first coated on a release substrate (**Figure 6**c). Then, a prepolymer solution is coated on top and fills the network. After solvent evaporation and polymerization, the

composite film is peeled off from the release substrate, along with the conductive network embedded under its surface. The precursor solution usually contains reactive liquid monomers and oligomers that can be cured with thermal or photo initiation. The advantage of curing monomers together with the conductive network is that if there are appropriate functional groups on the conductive materials, covalent or other strong bonds can form between the elastomer and the network. These strong interactions crucially ensure the complete transfer of conductive network from the release substrate.[94] A simple scotch tape test is usually adopted to evaluate the interaction.[95] Briefly, the conductive surface of the electrode is repeatedly attached to and released from sticky tapes. Ideally, the resistance changes little, indicating good interaction between the conductive materials and elastomer matrix. If the interaction is weak, conductive materials will be removed from the elastomer surface, along with significant resistance increase.

Metallic nanomaterials are the embedded conductive network material of choice. They have high conductivity comparable to bulk metal, and a low percolation threshold for softer mechanical properties. Metallic nanomaterials have different dimensions, including metallic nanoparticles (0-D),[96] nanowires (1-D),[97] and nanoflakes/nanosheet (2-D).[98] Among them, nanowires are reported to have 10 to 100 times lower percolation threshold than nanoparticles.[99] Owing to the long and thin shapes of nanowires, a great number of contact junctions can form per single nanowire in conductive networks. These contact junctions can be further welded by annealing,[100] plasma treating,[101] and mechanical pressing,[102] which boost the conductivity and mechanical stability of the network. Large openings among nanowires not

only allow visible light to pass through, but also benefit infiltration of precursor solution. Among various metallic nanowires, AgNW is the most prevalent materials to construct conductive networks and is found in many stretchable EL devices.[103] For example, Liang et al.[92a] mixed ethoxylated bisphenol A dimethacrylate monomer with siliconized urethane acrylate oligomer as precursor to infiltrate AgNWs network. After curing, AgNWs embedded in poly(urethane acrylate) (PUA) was peeled off from release substrate and used as electrode for PLEC devices. The AgNWs/PUA electrodes have high transparency (83% at 550 nm wavelength), high conductivity (15 Ω/sq), low roughness (peak to valley value of 3.4 nm), and high stretchability (maximum strain up to 150%) (**Figure 9**a). The mechanical loss factor of PUA matrix was measured around 0.26 at 1 Hz, indicating mild viscoelasticity behavior. The electrode resistance increased 23 times when stretched to 100% strain. The sheet resistance of the electrode raised to 65 Ω/sq after 1400 cycles repeated stretch and release cycles but recovered to 45 Ω/sq after half an hour idle time at the relaxed state. Stretchable PLECs were demonstrated where an emissive layer was sandwiched by two AgNWs/PUA electrodes. The emissive layer consisted of SuperYellow (SY), a PPV-derivative conjugate polymer, PEO as ionic conductor, and lithium trifluoromethane sulphonate (LiTf) as doped salt. The chemical structure of SuperYellow can be found in **Figure 10**c. The resultant device had similar viscoelasticity as PUA matrix and could be stretched up to 120% strain and survived after 1000 stretch-release cycles of 0 to 30% strain (**Figure 9**b). In another study by Kim et al.,[104] silica aerogel solution was spin-coated on AgNWs before PDMS precursor infiltration. It was believed that high surface-to-volume ratio of aerogel could provide strong van der Waals interaction between AgNWs and PDMS. Comparisons were made between electrodes with and

without aerogel. In AFM images, AgNWs/PDMS show non-uniform surface with peak to valley roughness of 41 nm. While for AgNWs/aerogel/PDMS, the value is 17 nm. Sheet resistance of 15 Ω/sq was achieved with transmittance of 80% at 550 nm wavelength. This electrode was stretched up to 70%, with sheet resistance increased to 90 Ω/sq. Cyclic stretch and release of 100 cycles up to 25% strain raised sheet resistance to 27 Ω/sq.

Metallic CNTs are another frequently used conductive material in embedding structures.[105] Although formed CNT networks are less conductive than AgNWs, they have better chemical stability, especially in acid environment.[106] Yu et al.[61] embedded CNTs in a poly(tert-butyl acrylate) (PtBA) matrix. PtBA is a shape-memory polymer of low glass transition temperature ($T_g \approx 56$ °C). When heated to 70 °C, the CNTs/PtBA electrode could be stretched to 50% strain. A transmittance was 87% at 550 nm wavelength with 500 Ω/sq sheet resistance was achieved (**Figure 9**c). Thanks to the embedded structure and good interaction between CNTs and PtBA, the average surface roughness of this composite electrode is less than 10 nm. After 14 cycles of repeated stretch and release at 40% strain, the sheet resistance increase by 14%. Interestingly, the resistance reduced to the original value after annealing at 70 °C for 24 hours, indicating good, reversible bonding between CNTs and PtBA. The resistance increase during cyclic stretching could be attributed to the viscoelasticity of the PtBA. Stretchable LECs were fabricated by sandwiching emissive layers in between two PtBA/CNTs electrodes. The emissive layer consisted of polyfluorene copolymer, PEO-dimethacrylate ether, and LiTf. The resultant device showed maximum stretchability of 45% strain (**Figure 9**d). Turn-on voltage of 4.8 V, maximum current efficiency of 1.16 cd/A, and maximum brightness of 200 cd/m^2 at

11 V were achieved.

CNT/elastomer electrodes can also be used in ACEL devices. In another work, Son et al.[10b] embedded CNTs in a self-healing polymer matrix and demonstrated light-emitting capacitors. A self-healing polymer was synthesized by incorporating strong bonding unit, 4,4′-methylenebis(phenylurea) (MPU), and weak bonding unit, isophorone bisurea (IU), into the PDMS backbone. The resultant PDMS-$MPU_{0.4}$-$IU_{0.6}$ exhibited superior stretchability up to 1600% strain. The CNTs/PDMS-$MPU_{0.4}$-$IU_{0.6}$ electrode can bear 50% strain without significant electrical degradation. If the electrode was completely cut into two pieces and then brought together, after 24 hours at room temperature the resistance of the recovered film only increased by 17% compared with the original value (**Figure 9**e). The recovered electrode provided almost identical stress-strain behavior as the pristine one. For the ACEL device, ZnS:Cu phosphors were blended with PDMS-$MPU_{0.4}$-$IU_{0.6}$ and used as the emissive layer, which was sandwiched by two CNTs/PDMS-$MPU_{0.4}$-$IU_{0.6}$ electrodes. It is believed that the interlayer hydrogen bonding facilitated device assembly. The resultant device could be stretched up to 250% strain and endure 100 cycles of repeated stretch and release at 50% strain (**Figure 9**f).

4.2 Stretchable emissive layers:

Balancing stretchability and EL performance of emissive materials in intrinsically stretchable EL device is still the main challenge in this field. Unlike stretchable electrode whose mild resistance increase along with strain is somehow tolerable, the EL performance of stretchable

emissive layers could be hugely degraded under stretching. Without specific molecular design or introduction of elastic components, the device might easily short due to crack or void formed on the thin EL layer during stretching. So far, there are mainly two strategies for applying stretchable emissive layers: 1) synthesizing new intrinsically stretchable EL materials (basically stretchable EL conjugated polymer), and 2) blending additives to available EL materials that enhance overall stretchability. In this section, we discuss some commonly used stretchable emissive layers along with their device categories and processing methods.

4.2.1 Stretchable EL conjugated polymers

To search for appropriate stretchable EL materials for intrinsically stretchable EL devices, conjugated polymers of suitable bandgap are considered.[107] These polymers have been widely used in flexible PLEDs and PLECs.[108] Conjugated polymers transport charge carriers through π-electron delocalization on the contiguous sp^2 hybridized orbits. The extended intra-chain π-π conjugation and inter-chain π-π stacking leads to rigidity and limits their stretchability. Some conjugated polymers of high molecular weight allow a certain degree of elongation as tangled chains align during stretching. For example, Liang et al.[92b] employed a white light-emitting polymer together with 1,3-bis[(4-tert-butylphenyl)-1,3,4-oxidiazolyl]phenylene (OXD-7) as the thin film emissive layer in an intrinsically stretchable PLED. In this work, AgNWs were welded with graphene oxide (GO) and embedded in PUA matrix as the electrodes. PEDOT:PSS and polyethylenimine (PEI) were coated on two AgNWs-GO/PUA electrodes as the HTL and the ETL, respectively. After spin-coating the emissive layer on PEDOT:PSS, a lamination process was applied to finish device fabrication. Turn-on voltage of 7 V, maximum brightness

of 1100 cd/m^2 at 21 V, and maximum current efficiency of 4 cd/A were achieved. The resultant device could be stretched up to 130% strain and endure 100 cycles of repeated stretch and release at 40% strain.

The essential contradict of conjugated polymers remains between their extended π-π conjugation nature and high stretchability needs. To improve stretchability, molecular engineering is necessary to modify the backbone and sidechains of conjugated polymers, where stretchable blocks can be introduced.[69, 109] Molecule engineering can also alter the T_g and the inter-chain interaction of target polymers. Nevertheless, it is still challenging to manipulate the stretchability without affecting electrical and optic properties of the original materials. So far, there are quite a few reports about stretchable conjugated polymers, while most of them are not EL materials.[110] Intrinsically stretchable, high-performance light-emitting conjugated polymers are still under development. Hsieh et al.[111] synthesized a stretchable blue light-emitting rod-coil conjugated polymer, poly[2,7-(9,9-dihexylfluorene)]-block-poly(n-butyl acrylate) (PF-b-PBA). PF was known as a high-performance blue light-emitting conjugated polymer of high PLQY, and high thermal stability. PBA served as a low T_g (−60.0 °C) elastomer that increased the deformability of block copolymers. As expected, phase separation occurred due to the incompatibility between PBA segments and PF segments. A special self-assembled nanofibrillar structure could be observed by AFM. By controlling the ratio between PF and PBA, annealed PF_{4k}-b-PBA_{7k} thin film exhibited stable blue PL under 100% strain, and the thin film morphology remained stable. In another work, Jao et al.[112] also adopted PF as the light emitting segments but applied poly(isoprene) (PI) as the elastic strand in the block

copolymer. PI is a soft elastomer and has T_g as low as -72 °C. By controlling the ratio between PF (rod segments) and PI (coil segments), the PF_{12K}-b-PI_{5K} copolymer could be stretched up to 150% strain with a few nanoscale cracks. Under 100% strain, the PL emission spectrum of PF_{12K}-b-PI_{5K} thin film remained stable, while PF_{18K}-b-PI_{5K} thin film exhibited an obvious reduction on emission peak intensity. This implied that a certain weight fraction of elastic PI segments was necessary to absorb the stress during stretching. This EL material was used to fabricate a stretchable PLED, where PEDOT:PSS was coated on PU as anode. Eutectic galliumindium (EGaIn) was coated on PF_{12K}-b-PI_{5K} thin film as cathode. Brightness of 70 cd/m^2 was achieved when biased at 10 V. The device could be stretched up to 140% strain and provided nominal luminance after 100 cycles of repeated stretch and release at 50% strain.

Today, most of the stretchable EL layers within intrinsically stretchable EL devices are blends of EL materials and additives. Compared with molecularly engineering and synthesizing new conjugated polymers, mixing available EL material with additives is straightforward. Commonly blended EL materials include conjugated polymers,[113] perovskite crystals,[114] and ZnS phosphors.[115] The additives in the blends could be small molecules that lubricate or the polymer chains, high molecular weight polymers of low T_g that allow certain degree of elongation, or highly stretchable elastomers. In general, to fabricate stretchable EL devices, EL materials and additives are firstly co-dissolved in solvents or the liquid monomers of desired elastomers, following by spin-casting and drying/curing to form stretchable EL thin layers. In the following paragraphs, various stretchable emissive blends are discussed according with their fabrication methods and device categories.

4.2.2 EL conjugated polymer with surfactants

It is a common practice to increase the mechanical compliancy of polymers by adding plasticizers and other low melting point compounds. For PLEDs, the additives in the emissive polymer should not hinder charge transport, recombination, or quench PLQY. In the fabrication of stretchable PLEDs, one has to also consider the solubility of the additive in a common solvent, and impact of the additive and the emissive polymer by the solvent of the layers spin-coated subsequently on top of the emissive layer. Finding a suitable orthogonal solvent is often a major challenge in the fabrication of PLEDs by successive depositions. Alternatively, the following semiconductive layers or the top electrode could be pre-formed on a separate, release substrate and transfer laminated onto the emissive layer. This approach decreases the fabrication yield as the process could introduce trapped air-bubbles, and the lamination pressure can introduce defects in the semiconductor layers due to surface roughness of the laminated films and the laminator rolls.

Recently, Kim et al.[113] blended SY with Triton X, a non-ionic surfactant, as the stretchable emissive layer. It was suggested that Triton X served as a plasticizer and increased the free-volume in SY. Specifically, the Triton molecules occupy space among adjacent chains of SY and alters the coiled configuration to linear conformation. Interestingly, although Triton X is an insulator, when the weight ratio between SY and Triton X is 2:1, the electron and hole mobility of SY-Triton film is slightly higher than that of pristine SY film. In addition, the polymer's Young's modulus decreased from 412 MPa to 77 MPa, the crack onset strain

increased from 40% to 80%, and the T_g decreased from 82.1℃ to 55.2 ℃. These changes were attributed to the conformational change of SY. In this work, PEDOT:PSS was also blended with Triton X to increase its stretchability. The PLED was fabricated by subsequently spin-coating PEDOT:PSS-Triton X, SY-Triton X, ZnO NPs, doped polyethyleneimine ethoxylated (d-PEIE), and AgNWs (**Figure 10**a). Additional ZnO and d-PEIE layers were deposited on the AgNW layer to facilitate charge injection. The resultant device had turn-on voltage of 8.3 V, maximum current efficiency of 1.6 cd/A, and maximum brightness of 4400 cd/m^2 at 11 V. The device could be stretched up to 80% strain, with 200 cycles of repeated stretch and release at 40% strain (**Figure 10**b).

4.2.3 EL conjugated polymers with ionic conductors

Ionic conductors resemble plasticizers with regard to low volatility and fluid-like mechanical properties. For stretchable LECs, ionic conductors are essentially blended with EL materials in the emissive layers.[116] Due to excluded volume in polymers, phase separation can be observed in the emissive layer in PLECs, where domains of conjugated polymers and ionic conductors are separated from each other but evenly distributed across the film. Ideally, the mobile ions can diffuse in the conjugated polymer domain to induce electrochemical doping. A large domain size could negatively affect the doping efficacy due to uneven electric field distribution. On the other hand, electrons and holes need to transport to reach each other and recombine, indicating that the conjugated polymer domain needs to form a continuous pathway between the electrodes. When the ionic conductors fill the pores of continuous conjugated polymer

phase and form interpenetrating microstructure, the emissive layer appears like a "water soaked sponge" and can hold its functionality during stretching.[117]

To co-dissolve the EL conjugated polymer and ionic conductors, the solvents usually have strong dissolving ability. Spin coating onto a stretchable electrode requires extra attention as the strong solvent could attack the electrode material or its substrate. As such, it is also common to coat the emissive layers on a release substrate and transfer them onto stretchable TCEs. The opposite electrode is spin-coated or laminated on emissive layer to finish the device fabrication.

Yan et al.[118] synthesized a supramolecular polymer materials that consisted of polytetramethylene glycol, tetraethylene glycol soft domains and reversible quadruple H-bonding cross-linkers. This material was employed by Liu et al.[119] as the ionic conductor in the emissive layer of stretchable PLECs (**Figure 10**c). The emissive layer also consisted of SY, lithium triflate, and ethoxylated trimethylopropane triacrylate that can be polymerized by heating. The ratio between SY and the ionic conductor was optimized to 1:1, and the resultant PLEC can endure 20 cycles of repeated stretch and release at 30% strain (**Figure 10**d).

The EL materials for LECs are not restricted to conjugated polymers. Ionic iridium-based transition metal complexes (iTMCs) are also appropriate candidates. For iTMCs that are both ionic and electronic conductive, additional ionic conductor might not be necessary. In this case, iTMCs can be directly mixed with elastomer to form the stretchable emissive layer. Filiatrault et al.[120] dispersed $Ru(dtb\text{-}bpy)_3^{2+}(PF_6)^-_2$ (dtb-bpy = 4,4′-di-tert-butyl-2,2′-dipyridyl) within

PDMS as the emissive layer and demonstrated a stretchable LEC. The volume fraction of PDMS was 25%. Optical microscope images indicated that the PDMS filled the pinholes on the pristine $Ru(dtb\text{-}bpy)_3^{2+}(PF_6)^{-}_2$ film and exhibited clear phase separation between $Ru(dtb\text{-}bpy)_3^{2+}(PF_6)^{-}_2$ domains and PDMS domains. According to AFM images, the root-mean-square surface roughness of the $Ru(dtb\text{-}bpy)_3^{2+}(PF_6)^{-}_2$/PDMS film was merely 4.54 nm, which was acceptable in LECs. To fabricate the device, gold was evaporated on PDMS as stretchable TCEs. After spin-coating the emissive layer on the gold electrode, EGaIn was deposited as the cathode (**Figure 10**e). The maximum stretchability of the device was 27% strain (**Figure 10**f). After 50 stretch-release cycles the total emitted photon radiance dropped one order of magnitude.

4.2.4 ZnS phosphors elastomer composites

The EL materials in ACEL devices are dominated by ZnS phosphor powders and their alloys.[121] ZnS phosphors are generally doped with trace amount of dopant ions such as Ag^{+}, Mn^{2+}, and Cu^{+} to tune the color of the emitted light. These dopants also called activators, which are impurities in the ZnS lattice, and serve as the luminescent centers when electric field is applied.[122] Some of these dopants can be slowly oxidized or react with moisture, which is a main cause for ACEL devices performance degradation.[123] Fortunately, in most of the stretchable ACEL devices, the phosphors powers (diameter around 20 μm) are buried within a thick elastomer layer (from hundreds of μm to a few millimeters). The phosphor powder and the matrix forming polymer (or its precursor) are dispersed in an organic solvent, and cast to form the thick emissive layer via spin-coating,[124] blade-coating,[125] or lamination[126] to

fabricate stretchable ACEL devices. ACEL fibers might be fabricated via repeatedly dip-coating[58c] and co-extrusion.[78, 80] Silicone elastomers such as Sylgard-184 and Ecoflex are popular choices for blending the phosphors. ZnS phosphors can be easily dispersed in the silicone resins without extra additives or ligands. Owing to such facile blending process, the combination of ZnS phosphor powers plus silicone was almost the exclusive choice to form the emissive layers in stretchable ACEL devices in the early years.[58c, 67a, 90, 124]

However, the dielectric constant of PDMS is merely 2.72 (measure at 100 Hz). In fact, a vast majority of polymers have small dielectric constant between 2 to 5.[127] To focus electrical field on phosphor powders, a high dielectric constant elastomer is desired (**Figure 11**a). Thus, many efforts have been spent on designing, synthesizing, and mixing high dielectric constant elastomer with ZnS phosphors in stretchable ACEL devices.[128] For example, Stauffer et al.[23] added barium titanate ($BaTiO_3$) particles in the ZnS:Cu-PDMS dispersion. In this structure, small BaTiO3 particles (diameter~500 nm) filled the voids among large ZnS:Cu particles (diameter ~ 7 μm), and the voids among these two particles were further infiltrated by PDMS precursor (**Figure 11**b). The dielectric constant of the resulting $BaTiO_3$-ZnS:Cu-PDMS composite was tripled than that of pristine PDMS in all frequency range (10 Hz to 10^5 Hz). The ACEL device consisting of AgNWs/PDMS electrodes and $BaTiO_3$-ZnS:Cu-PDMS emissive layer exhibited maximum brightness of 121 cd/m^2, while the control device without $BaTiO_3$ in the emissive layer only produced 16 cd/m^2 brightness under the same driving condition (250 V, 2.2k Hz) (**Figure 11**c). The device normally failed when stretched by greater than 80% -110% strain. It endured 50% areal strain and 500 stretch-release cycles at 50% tensile strain.

Zhou et al.,[129] employed a polar thermoplastic elastomer, elastomer-poly-((vinylidene fluoride)-hexafluoropropylene) (e-PVDF-HFP), to embed the ZnS:Cu powder as the emissive layer. The e-PVDF-HFP exhibited dielectric constant larger than 10 at 10 kHz. They also used fine phosphor powers (average dimension ~ 2.6 μm) to lower the EL layer thickness and driving voltage. To ensure the homogenous distribution of ZnS:Cu in e-PVDF-HFP, the elastomer were firstly dissolved in a co-solvent of tetrahydrofuran and dimethylformamide. ZnS:Cu powders were added with a 1:2 weight ratio of the elastomer. After solvent evaporation, the slurry was homogenized by passing it through a three-roll mill for 5 times. The ACEL device was fabricated through a lamination process where the e-PVDF-HFP-ZnS:Cu emissive layer was sandwiched by two AgNWs/thermoplastic polyurethane (TPU) electrodes (**Figure 11**d). The maximum brightness was 785 cd/m^2 when driven at 180V, 20k Hz. The device could be uniaxially stretched to 100% strain, and 47% strain in area. The emission intensity retained 81% of the original state after the device being repeatedly stretched and released for 500 cycles at 50% strain. The devices remained functional when being punctured with a needle, partially cut, and poked with a hole (**Figure 11**e).

5. Conclusion

Various light emitting devices, including LEDs, LECs, and ACEL, have all been adapted for stretchable EL devices through either stretchable structures or stretchable materials. In the structure-enabled approach, stretchable architectures have been designed that allow for large global deformation while the individual EL units undergo minimal stretching. The island-

bridge structures, buckling structures, and textile structures have their distinctive requirements for EL units and device fabrication processes, and will likely be suitable for different application schemes. Meanwhile, other structures like origami/kirigami-inspired[40b], mesh, and spring-like structures are also interesting to be used in structure-enabled stretchable EL device. The development of materials-enabled stretchable EL devices entails stretchable TCEs and EL materials. Ionically conductive gels, transparent conductive thin coating on elastomer substrate, and transparent conductive network embedded in elastomer are three stretchable TCEs achieving proper compromise in conductivity, optical transmittance, and stretchability. Inherently stretchable EL conjugated polymers are rare, blending with plasticizing surfactants and ionic conductors show promise to enhance the stretchability while retaining, or in certain cases, enhancing the EL performance of the pristine polymers. The solution processing of the polymers is both a blessing and a curse: solution processing is relatively easy to start up and scale up. However, the solvents in the subsequent processing steps may attack the layers already formed. Lamination may circumvent this problem, though it may introduce new defects in the EL layers. Going forward, new TCEs are required that not only offer high stretchability, high surface conductivity, and optical transparency, but are also resistant against solvents and treatment temperatures. Future work should also focus on the EL performance of the stretchable EL materials, including improving the luminous efficiency and operational stability of the PLECs, increasing brightness and reducing operation voltage of the ACEL devices.

Acknowledgements

The authors wish to acknowledge partial finance support from the UC-Mexus Conacyt Collaborative Grants Program and the UCLA Summer Mentored Research Fellowship (SMRF) program. This work is dedicated to Professor Daoben Zhu on the Occasion of his 80th Birthday.

Conflict of Interest

The authors declare no conflict of interest.

Author biographies

Hexing Yin is a Ph.D. candidate at the Department of Materials Science and Engineering, UCLA, working on the fabrication of stretchable displays in the UCLA Soft Materials Research Laboratory. He received his B.S. (2016) degrees from the School of Chemistry and Chemical Engineering at Nanjing University.

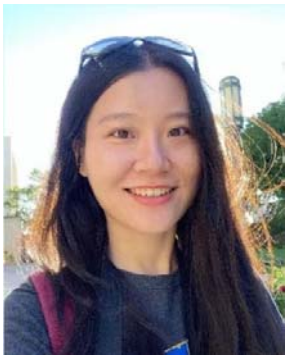

Yuan Zhu got her B.S. degree in chemical and biomolecular engineering from UCLA. Now she is a PhD student in the UCLA Soft Materials Research Laboratory. Her research interests focus on stretchable electroluminescence devices and silver nanowire composites for electronics application.

Qibing Pei is Professor of Materials Science and Engineering and Mechanical Engineering at the University of California, Los Angeles. He specializes in synthetic polymers and composites for electronic, electromechanical, and photonic applications. He received a PhD from the Institute of Chemistry, Chinese Academy of Sciences. He was a postdoctoral fellow in Linköping University and worked at UNIAX Corporation (now DuPont Display) and SRI International. Since 2004, he is a full professor directing the UCLA Soft Materials Research Laboratory. He is a Fellow of SPIE, member of ACS and MRS, Associate Editor of Smart

Materials & Structures and Soft Robotics, and Advisory Board Member of Advanced Electronic Materials and Scientific Reports.

Reference

[1] N. Bowden, S. Brittain, A. G. Evans, J. W. Hutchinson, G. M. Whitesides, *Nature* **1998**, 393, 146.

[2] D. H. Kim, J. H. Ahn, W. M. Choi, H. S. Kim, T. H. Kim, J. Song, Y. Y. Huang, Z. Liu, C. Lu, J. A. Rogers, *Science* **2008**, 320, 507.

[3] S. Wang, J. Xu, W. Wang, G. N. Wang, R. Rastak, F. Molina-Lopez, J. W. Chung, S. Niu, V. R. Feig, J. Lopez, T. Lei, S. K. Kwon, Y. Kim, A. M. Foudeh, A. Ehrlich, A. Gasperini, Y. Yun, B. Murmann, J. B. Tok, Z. Bao, *Nature* **2018**, 555, 83.

[4] T. Yamada, Y. Hayamizu, Y. Yamamoto, Y. Yomogida, A. Izadi-Najafabadi, D. N. Futaba, K. Hata, *Nat Nanotechnol* **2011**, 6, 296.

[5] R. Pelrine, R. Kornbluh, Q. Pei, J. Joseph, *Science* **2000**, 287, 836.

[6] S. Xu, Y. Zhang, J. Cho, J. Lee, X. Huang, L. Jia, J. A. Fan, Y. Su, J. Su, H. Zhang, H. Cheng, B. Lu, C. Yu, C. Chuang, T. I. Kim, T. Song, K. Shigeta, S. Kang, C. Dagdeviren, I. Petrov, P. V. Braun, Y. Huang, U. Paik, J. A. Rogers, *Nat Commun* **2013**, 4, 1543.

[7] S. I. Park, Y. Xiong, R. H. Kim, P. Elvikis, M. Meitl, D. H. Kim, J. Wu, J. Yoon, C. J. Yu, Z. Liu, Y. Huang, K. C. Hwang, P. Ferreira, X. Li, K. Choquette, J. A. Rogers, *Science* **2009**, 325, 977.

[8] Z. Huang, Y. Hao, Y. Li, H. Hu, C. Wang, A. Nomoto, T. Pan, Y. Gu, Y. Chen, T. Zhang, W. Li, Y. Lei, N. Kim, C. Wang, L. Zhang, J. W. Ward, A. Maralani, X. Li, M. F. Durstock, A. Pisano, Y. Lin, S. Xu, *Nat. Electron.* **2018**, 1, 473.

[9] D. Chen, Q. Pei, *Chem Rev* **2017**, 117, 11239.

[10] a) V. Arumugam, M. D. Naresh, R. Sanjeevi, *J. Biosci.* **1994**, 19, 307. b) D. Son, J. Kang, O. Vardoulis, Y. Kim, N. Matsuhisa, J. Y. Oh, J. W. To, J. Mun, T. Katsumata, Y. Liu, A. F. McGuire, M. Krason, F. Molina-Lopez, J. Ham, U. Kraft, Y. Lee, Y. Yun, J. B. Tok, Z. Bao, Nat Nanotechnol 2018, 13, 1057.

[11] C. Huang-Jen, C. Shih-Jen, *IEEE Trans. Ind. Electron.* **2007**, 54, 2751.

[12] a) X. Zhou, P. Tian, C.-W. Sher, J. Wu, H. Liu, R. Liu, H.-C. Kuo, *Prog. Quantum. Electron.* **2020**, 71, 100263; b) H. E. Lee, J. H. Shin, J. H. Park, S. K. Hong, S. H. Park, S. H. Lee, J. H. Lee, I. S. Kang, K. J. Lee, *Adv. Funct. Mater.* **2019**, 29, 1808075.

[13] G. Gustafsson, Y. Cao, G. M. Treacy, F. Klavetter, N. Colaneri, A. J. Heeger, *Nature* **1992**, 357, 477.

[14] a) Y.-F. Li, X. Liu, J. Feng, Y. Xie, F. Zhao, X.-L. Zhang, Q. Pei, H.-B. Sun, *Nanophotonics* **2020**, 9, 3567; b) D. Kim, T. Yokota, T. Suzuki, S. Lee, T. Woo, W. Yukita, M. Koizumi, Y. Tachibana, H. Yawo, H. Onodera, M. Sekino, T. Someya, *Proc Natl Acad Sci U S A* **2020**, 117, 21138; c) M. Choi, S. R. Bae, L. Hu, A. T. Hoang, S. Y. Kim, J. H. Ahn, *Sci. Adv.* **2020**, 6, eabb5898; d) T. Y. Zhao, D. D. Zhang, T. Y. Qu, L. L. Fang, Q. B. Zhu, Y. Sun, T. H. Cai, M. L. Chen, B. W. Wang, J. H. Du, W. C. Ren, X. Yan, Q. W. Li, S. Qiu, D. M. Sun, *ACS Appl. Mater. Interfaces* **2019**, 11, 11699.

[15] a) N. Sun, C. Jiang, Q. Li, D. Tan, S. Bi, J. Song, *J. Mater. Sci.: Mater. Electron.* **2020**, 31, 20688; b) D. C. Kim, H. J. Shim, W. Lee, J. H. Koo, D. H. Kim, *Adv. Mater.* **2020**, 32, e1902743; c) J. H. Koo, D. C. Kim, H. J. Shim, T.-H. Kim, D.-H. Kim, *Adv. Funct. Mater.* **2018**, 28, 1801834.

[16] H. Zhang, J. A. Rogers, *Adv. Opt. Mater.* **2019**, 7, 1800936.

[17] Y. F. Li, J. Feng, H. B. Sun, *Nanoscale* **2019**, 11, 19119.

[18] T. H. Le, Y. Choi, S. Kim, U. Lee, E. Heo, H. Lee, S. Chae, W. B. Im, H. Yoon, *Adv. Opt. Mater.* **2020**, 8, 1901972.

[19] Y. F. Li, S. Y. Chou, P. Huang, C. Xiao, X. Liu, Y. Xie, F. Zhao, Y. Huang, J. Feng, H. Zhong, H. B. Sun,

Q. Pei, *Adv. Mater.* **2019**, 31, e1807516.
[20] a) Q. Pei, G. Yu, C. Zhang, Y. Yang, A. J. Heeger, *Science* **1995**, 269, 1086; b) Q. Pei, Y. Yang, G. Yu, C. Zhang, A. J. Heeger, *J. Am. Chem. Soc.* **1996**, 118, 3922.
[21] Q. Pei, Y. Yang, G. Yu, Y. Cao, A. J. Heeger, *Synth. Met.* **1997**, 85, 1229.
[22] S. van Reenen, P. Matyba, A. Dzwilewski, R. A. Janssen, L. Edman, M. Kemerink, *J Am Chem Soc* **2010**, 132, 13776.
[23] F. Stauffer, K. Tybrandt, *Adv. Mater.* **2016**, 28, 7200.
[24] D. R. Vij, *Handbook of Electroluminescent Materials*, Institute of Physics Publishing, London, UK **2004**.
[25] Z. Yang, W. Wang, J. Pan, C. Ye, *Cell Reports Physical Science* **2020**, 1, 100213.
[26] a) T. Sekitani, H. Nakajima, H. Maeda, T. Fukushima, T. Aida, K. Hata, T. Someya, *Nat Mater* **2009**, 8, 494; b) R. H. Kim, D. H. Kim, J. Xiao, B. H. Kim, S. I. Park, B. Panilaitis, R. Ghaffari, J. Yao, M. Li, Z. Liu, V. Malyarchuk, D. G. Kim, A. P. Le, R. G. Nuzzo, D. L. Kaplan, F. G. Omenetto, Y. Huang, Z. Kang, J. A. Rogers, *Nat Mater* **2010**, 9, 929.
[27] J. A. Rogers, T. Someya, Y. Huang, *Science* **2010**, 327, 1603.
[28] Y. Zhang, H. Fu, S. Xu, J. A. Fan, K.-C. Hwang, J. Jiang, J. A. Rogers, Y. Huang, *J. Mech. Phys. Solids* **2014**, 72, 115.
[29] X. Hu, P. Krull, B. de Graff, K. Dowling, J. A. Rogers, W. J. Arora, *Adv. Mater.* **2011**, 23, 2933.
[30] P. Lee, J. Lee, H. Lee, J. Yeo, S. Hong, K. H. Nam, D. Lee, S. S. Lee, S. H. Ko, *Adv. Mater.* **2012**, 24, 3326.
[31] M. S. Lim, M. Nam, S. Choi, Y. Jeon, Y. H. Son, S. M. Lee, K. C. Choi, *Nano Lett* **2020**, 20, 1526.
[32] a) J. Byun, B. Lee, E. Oh, H. Kim, S. Kim, S. Lee, Y. Hong, *Sci. Rep.* **2017**, 7, 45328; b) M. Choi, B. Jang, W. Lee, S. Lee, T. W. Kim, H.-J. Lee, J.-H. Kim, J.-H. Ahn, *Adv. Funct. Mater.* **2017**, 27, 1606005.
[33] A. Romeo, Q. Liu, Z. Suo, S. P. Lacour, *Appl. Phys. Lett.* **2013**, 102, 131904.
[34] I. M. Graz, D. P. J. Cotton, A. Robinson, S. P. Lacour, *Appl. Phys. Lett.* **2011**, 98, 124101.
[35] S. P. Lacour, S. Wagner, R. J. Narayan, T. Li, Z. Suo, *J. Appl. Phys.* **2006**, 100, 014913.
[36] A. Robinson, A. Aziz, Q. Liu, Z. Suo, S. P. Lacour, *J. Appl. Phys.* **2014**, 115, 143511.
[37] M. Drack, I. Graz, T. Sekitani, T. Someya, M. Kaltenbrunner, S. Bauer, *Adv. Mater.* **2015**, 27, 34.
[38] T. Kim, H. Lee, W. Jo, T. S. Kim, S. Yoo, *Adv. Mater. Technol.* **2020**, 5, 2000494.
[39] a) X. Guo, X. Ni, J. Li, H. Zhang, F. Zhang, H. Yu, J. Wu, Y. Bai, H. Lei, Y. Huang, J. A. Rogers, Y. Zhang, *Adv. Mater.* **2021**, 33, e2004919; b) Y. Hong, B. Lee, E. Oh, J. Byun, *Information Display* **2017**, 33, 6.
[40] a) S. Kim, J. Byun, S. Choi, D. Kim, T. Kim, S. Chung, Y. Hong, *Adv. Mater.* **2014**, 26, 3094; b) J.-H. Hong, J. M. Shin, G. M. Kim, H. Joo, G. S. Park, I. B. Hwang, M. W. Kim, W.-S. Park, H. Y. Chu, S. Kim, *J. Soc. Inf. Disp* **2017**, 25, 194.
[41] K. Li, X. Cheng, F. Zhu, L. Li, Z. Xie, H. Luan, Z. Wang, Z. Ji, H. Wang, F. Liu, Y. Xue, C. Jiang, X. Feng, L. Li, J. A. Rogers, Y. Huang, Y. Zhang, *Adv. Funct. Mater.* **2019**, 29, 1806630.
[42] M. S. White, M. Kaltenbrunner, E. D. Głowacki, K. Gutnichenko, G. Kettlgruber, I. Graz, S. Aazou, C. Ulbricht, D. A. M. Egbe, M. C. Miron, Z. Major, M. C. Scharber, T. Sekitani, T. Someya, S. Bauer, N. S. Sariciftci, *Nat. Photon* **2013**, 7, 811.
[43] T. Yokota, P. Zalar, M. Kaltenbrunner, H. Jinno, N. Matsuhisa, H. Kitanosako, Y. Tachibana, W. Yukita, M. Koizumi, T. Someya, *Sci. Adv.* **2016**, 2, e1501856.
[44] M. K. Choi, J. Yang, K. Kang, D. C. Kim, C. Choi, C. Park, S. J. Kim, S. I. Chae, T. H. Kim, J. H. Kim, T. Hyeon, D. H. Kim, *Nat Commun* **2015**, 6, 7149.
[45] A. Schweikart, A. Fery, *Microchimica Acta* **2009**, 165, 249.

[46] T. W. Kim, J. S. Lee, Y. C. Kim, Y. C. Joo, B. J. Kim, *Materials (Basel)* **2019**, 12.
[47] T. H. Kim, C. S. Lee, S. Kim, J. Hur, S. Lee, K. W. Shin, Y. Z. Yoon, M. K. Choi, J. Yang, D. H. Kim, T. Hyeon, S. Park, S. Hwang, *ACS Nano* **2017**, 11, 5992.
[48] D. Yin, N. R. Jiang, Y. F. Liu, X. L. Zhang, A. W. Li, J. Feng, H. B. Sun, *Light Sci. Appl.* **2018**, 7, 35.
[49] D. Yin, J. Feng, R. Ma, Y. F. Liu, Y. L. Zhang, X. L. Zhang, Y. G. Bi, Q. D. Chen, H. B. Sun, *Nat Commun* **2016**, 7, 11573.
[50] D. Yin, N. R. Jiang, Z. Y. Chen, Y. F. Liu, Y. G. Bi, X. L. Zhang, J. Feng, H. B. Sun, *Adv. Opt. Mater.* **2019**, 8, 1901525.
[51] D. Yin, J. Feng, N. R. Jiang, R. Ma, Y. F. Liu, H. B. Sun, *ACS Appl. Mater. Interfaces* **2016**, 8, 31166.
[52] S. Jeong, H. Yoon, B. Lee, S. Lee, Y. Hong, *Adv. Mater. Technol.* **2020**, 2000231.
[53] a) L. Wang, X. Fu, J. He, X. Shi, T. Chen, P. Chen, B. Wang, H. Peng, *Adv. Mater.* **2020**, 32, e1901971; b) S. Kwon, Y. H. Hwang, M. Nam, H. Chae, H. S. Lee, Y. Jeon, S. Lee, C. Y. Kim, S. Choi, E. G. Jeong, K. C. Choi, *Adv. Mater.* **2020**, 32, e1903488.
[54] Z. Zhang, X. Shi, H. Lou, Y. Xu, J. Zhang, Y. Li, X. Cheng, H. Peng, *J. Mater. Chem. C* **2017**, 5, 4139.
[55] Y. Wu, S. S. Mechael, C. Lerma, R. S. Carmichael, T. B. Carmichael, *Matter* **2020**, 2, 882.
[56] Y. J. Song, J. W. Kim, H. E. Cho, Y. H. Son, M. H. Lee, J. Lee, K. C. Choi, S. M. Lee, *ACS Nano* **2020**, 14, 1133.
[57] X. Shi, Y. Zuo, P. Zhai, J. Shen, Y. Yang, Z. Gao, M. Liao, J. Wu, J. Wang, X. Xu, Q. Tong, B. Zhang, B. Wang, X. Sun, L. Zhang, Q. Pei, D. Jin, P. Chen, H. Peng, *Nature* **2021**, 591, 240.
[58] a) S. Kwon, W. Kim, H. Kim, S. Choi, B.-C. Park, S.-H. Kang, K. C. Choi, *Adv. Electron. Mater* **2015**, 1, 1500103; b) Z. Zhang, K. Guo, Y. Li, X. Li, G. Guan, H. Li, Y. Luo, F. Zhao, Q. Zhang, B. Wei, Q. Pei, H. Peng, *Nat. Photon* **2015**, 9, 233; c) G. Liang, M. Yi, H. Hu, K. Ding, L. Wang, H. Zeng, J. Tang, L. Liao, C. Nan, Y. He, C. Ye, *Adv. Electron. Mater* **2017**, 3, 1700401.
[59] a) D. Hu, X. Xu, J. Miao, O. Gidron, H. Meng, *Materials (Basel)* **2018**, 11; b) Z. Zhang, X. Shi, H. Lou, X. Cheng, Y. Xu, J. Zhang, Y. Li, L. Wang, H. Peng, *J. Mater. Chem. C* **2018**, 6, 1328.
[60] S. Choi, H. Lee, R. Ghaffari, T. Hyeon, D. H. Kim, *Adv. Mater.* **2016**, 28, 4203.
[61] Z. Yu, X. Niu, Z. Liu, Q. Pei, *Adv. Mater.* **2011**, 23, 3989.
[62] Y. Q. Zheng, Y. Liu, D. Zhong, S. Nikzad, S. Liu, Z. Yu, D. Liu, H. C. Wu, C. Zhu, J. Li, H. Tran, J. B. Tok, Z. Bao, *Science* **2021**, 373, 88.
[63] a) S. P. Lacour, S. Wagner, Z. Huang, Z. Suo, *Appl. Phys. Lett.* **2003**, 82, 2404; b) D. R. Cairns, R. P. Witte, D. K. Sparacin, S. M. Sachsman, D. C. Paine, G. P. Crawford, R. R. Newton, *Appl. Phys. Lett.* **2000**, 76, 1425; c) W. Wu, *Sci. Technol. Adv. Mater* **2019**, 20, 187.
[64] a) Y. Chen, Y. Wu, S. S. Mechael, T. B. Carmichael, *Chem. Mater.* **2019**, 31, 1920; b) S. Choi, S. Kim, H. Kim, B. Lee, T. Kim, Y. Hong, *IEEE Sens. J.* **2020**, 20, 14655.
[65] M. K. Choi, J. Yang, D. C. Kim, Z. Dai, J. Kim, H. Seung, V. S. Kale, S. J. Sung, C. R. Park, N. Lu, T. Hyeon, D. H. Kim, *Adv. Mater.* **2018**, 30.
[66] Y.-H. Tak, K.-B. Kim, H.-G. Park, K.-H. Lee, J.-R. Lee, *Thin Solid Films* **2002**, 411, 12.
[67] a) C. Larson, B. Peele, S. Li, S. Robinson, M. Totaro, L. Beccai, B. Mazzolai, R. Shepherd, *Science* **2016**, 351, 1071; b) S. Li, B. N. Peele, C. M. Larson, H. Zhao, R. F. Shepherd, *Adv. Mater.* **2016**, 28, 9770.
[68] X. Shi, X. Zhou, Y. Zhang, X. Xu, Z. Zhang, P. Liu, Y. Zuo, H. Peng, *J. Mater. Chem. C* **2018**, 6, 12774.
[69] J. Y. Oh, Z. Bao, *Adv Sci (Weinh)* **2019**, 6, 1900186.
[70] a) P. Lee, J. Ham, J. Lee, S. Hong, S. Han, Y. D. Suh, S. E. Lee, J. Yeo, S. S. Lee, D. Lee, S. H. Ko, *Adv. Funct. Mater.* **2014**, 24, 5671; b) B. S. Kim, H. Kwon, H. J. Kwon, J. B. Pyo, J. Oh, S. Y. Hong, J. H. Park, K. Char, J. S. Ha, J. G. Son, S. S. Lee, *Adv. Funct. Mater.* **2020**, 30, 1910214.

[71] a) Y. Wang, C. Zhu, R. Pfattner, H. Yan, L. Jin, S. Chen, F. Molina-Lopez, F. Lissel, J. Liu, N. I. Rabiah, Z. Chen, J. W. Chung, C. Linder, M. F. Toney, B. Murmann, Z. Bao, *Sci. Adv.* **2017**, 3, e1602076; b) X. Fan, W. Nie, H. Tsai, N. Wang, H. Huang, Y. Cheng, R. Wen, L. Ma, F. Yan, Y. Xia, *Adv Sci (Weinh)* **2019**, 6, 1900813.
[72] J. Wang, C. Yan, G. Cai, M. Cui, A. Lee-Sie Eh, P. See Lee, *Adv. Mater.* **2016**, 28, 4490.
[73] D. W. Kim, G. Lee, M. Pal, U. Jeong, *ACS Appl. Mater. Interfaces* **2020**, 12, 41969.
[74] F. Xu, Y. Zhu, *Adv. Mater.* **2012**, 24, 5117.
[75] S. B. Park, J. W. Han, J. H. Kim, A. F. Wibowo, A. Prameswati, J. Park, J. Lee, M. W. Moon, M. S. Kim, Y. H. Kim, *Adv. Opt. Mater.* **2021**, 2002041.
[76] C. H. Yang, B. Chen, J. Zhou, Y. M. Chen, Z. Suo, *Adv. Mater.* **2016**, 28, 4480.
[77] C. Zhao, Y. Zhou, S. Gu, S. Cao, J. Wang, M. Zhang, Y. Wu, D. Kong, *ACS Appl. Mater. Interfaces* **2020**, 12, 47902.
[78] Z. Zhang, L. Cui, X. Shi, X. Tian, D. Wang, C. Gu, E. Chen, X. Cheng, Y. Xu, Y. Hu, J. Zhang, L. Zhou, H. H. Fong, P. Ma, G. Jiang, X. Sun, B. Zhang, H. Peng, *Adv. Mater.* **2018**, 30, e1800323.
[79] Y. J. Tan, H. Godaba, G. Chen, S. T. M. Tan, G. Wan, G. Li, P. M. Lee, Y. Cai, S. Li, R. F. Shepherd, J. S. Ho, B. C. K. Tee, *Nat Mater* **2020**, 19, 182.
[80] D. Liu, J. Ren, J. Wang, W. Xing, Q. Qian, H. Chen, N. Zhou, *J. Mater. Chem. C* **2020**, 8, 15092.
[81] N. Matsuhisa, X. Chen, Z. Bao, T. Someya, *Chem Soc Rev* **2019**, 48, 2946.
[82] A. Laskowska, A. Marzec, G. Boiteux, M. Zaborski, O. Gain, A. Serghei, *Polym. Int.* **2013**, 62, 1575.
[83] K. G. Cho, J. I. Lee, S. Lee, K. Hong, M. S. Kang, K. H. Lee, *Adv. Funct. Mater.* **2020**, 30, 1907936.
[84] N. Kaiser, *Appl Opt* **2002**, 41, 3053.
[85] O. Graudejus, P. Gorrn, S. Wagner, *ACS Appl. Mater. Interfaces* **2010**, 2, 1927.
[86] M. Vosgueritchian, D. J. Lipomi, Z. Bao, *Adv. Funct. Mater.* **2012**, 22, 421.
[87] D. J. Lipomi, J. A. Lee, M. Vosgueritchian, B. C. K. Tee, J. A. Bolander, Z. Bao, *Chem. Mater.* **2012**, 24, 373.
[88] S. G. R. Bade, X. Shan, P. T. Hoang, J. Li, T. Geske, L. Cai, Q. Pei, C. Wang, Z. Yu, *Adv. Mater.* **2017**, 29.
[89] P. Li, K. Sun, J. Ouyang, *ACS Appl. Mater. Interfaces* **2015**, 7, 18415.
[90] J. Wang, C. Yan, K. J. Chee, P. S. Lee, *Adv. Mater.* **2015**, 27, 2876.
[91] B. You, Y. Kim, B. K. Ju, J. W. Kim, *ACS Appl. Mater. Interfaces* **2017**, 9, 5486.
[92] a) J. Liang, L. Li, X. Niu, Z. Yu, Q. Pei, *Nat. Photon* **2013**, 7, 817; b) J. Liang, L. Li, K. Tong, Z. Ren, W. Hu, X. Niu, Y. Chen, Q. Pei, *ACS Nano* **2014**, 8, 1590; c) Y. Chen, R. S. Carmichael, T. B. Carmichael, *ACS Appl. Mater. Interfaces* **2019**, 11, 31210; d) Y. Lin, W. Yuan, C. Ding, S. Chen, W. Su, H. Hu, Z. Cui, F. Li, *ACS Appl. Mater. Interfaces* **2020**, 12, 24074.
[93] R. Ma, S. Y. Chou, Y. Xie, Q. Pei, *Chem Soc Rev* **2019**, 48, 1741.
[94] D. W. Kim, M. Kong, U. Jeong, *Adv. Sci.* **2021**, 2004170.
[95] a) Y. B. Shin, Y. H. Ju, H. J. Lee, C. J. Han, C. R. Lee, Y. Kim, J. W. Kim, *ACS Appl. Mater. Interfaces* **2020**, 12, 10949; b) D. H. Jiang, Y. C. Liao, C. J. Cho, L. Veeramuthu, F. C. Liang, T. C. Wang, C. C. Chueh, T. Satoh, S. H. Tung, C. C. Kuo, *ACS Appl. Mater. Interfaces* **2020**, 12, 14408.
[96] A. Desireddy, B. E. Conn, J. Guo, B. Yoon, R. N. Barnett, B. M. Monahan, K. Kirschbaum, W. P. Griffith, R. L. Whetten, U. Landman, T. P. Bigioni, *Nature* **2013**, 501, 399.
[97] L. Hu, H. S. Kim, J.-Y. Lee, P. Peumans, Y. Cui, *ACS Nano* **2010**, 4, 2955.
[98] M. Mazur, *Electrochem. Commun.* **2004**, 6, 400.
[99] Y. Kim, J. Zhu, B. Yeom, M. Di Prima, X. Su, J.-G. Kim, S. J. Yoo, C. Uher, N. A. Kotov, *Nature* **2013**,

500, 59.
[100] a) M. Lagrange, D. P. Langley, G. Giusti, C. Jimenez, Y. Brechet, D. Bellet, *Nanoscale* **2015**, 7, 17410; b) D. P. Langley, M. Lagrange, G. Giusti, C. Jimenez, Y. Brechet, N. D. Nguyen, D. Bellet, *Nanoscale* **2014**, 6, 13535.
[101] J. Li, Y. Tao, S. Chen, H. Li, P. Chen, M.-z. Wei, H. Wang, K. Li, M. Mazzeo, Y. Duan, *Sci. Rep.* **2017**, 7.
[102] S. J. Lee, Y.-H. Kim, J. K. Kim, H. Baik, J. H. Park, J. Lee, J. Nam, J. H. Park, T.-W. Lee, G.-R. Yi, J. H. Cho, *Nanoscale* **2014**, 6, 11828.
[103] S. Hong, S. Lee, D.-H. Kim, *Proc. IEEE* **2019**, 107, 2185.
[104] J. Kim, J. Park, U. Jeong, J.-W. Park, *J. Appl. Polym. Sci.* **2016**, 133.
[105] M. F. De Volder, S. H. Tawfick, R. H. Baughman, A. J. Hart, *Science* **2013**, 339, 535.
[106] J. Zaumseil, *Semicond. Sci. Technol.* **2015**, 30, 074001.
[107] L. Akcelrud, *Prog. Polym. Sci.* **2003**, 28, 875.
[108] a) Z. Yu, L. Hu, Z. Liu, M. Sun, M. Wang, G. Grüner, Q. Pei, *Appl. Phys. Lett.* **2009**, 95, 203304; b) Z. Yu, M. Wang, G. Lei, J. Liu, L. Li, Q. Pei, *J. Phys. Chem. Lett.* **2011**, 2, 367; c) J. Liang, L. Li, X. Niu, Z. Yu, Q. Pei, *J. Phys. Chem. C* **2013**, 117, 16632.
[109] H. Tran, V. R. Feig, K. Liu, Y. Zheng, Z. Bao, *Macromolecules* **2019**, 52, 3965.
[110] a) J. Xu, S. Wang, G. N. Wang, C. Zhu, S. Luo, L. Jin, X. Gu, S. Chen, V. R. Feig, J. W. To, S. Rondeau-Gagne, J. Park, B. C. Schroeder, C. Lu, J. Y. Oh, Y. Wang, Y. H. Kim, H. Yan, R. Sinclair, D. Zhou, G. Xue, B. Murmann, C. Linder, W. Cai, J. B. Tok, J. W. Chung, Z. Bao, *Science* **2017**, 355, 59; b) G.-J. N. Wang, A. Gasperini, Z. Bao, *Adv. Electron. Mater* **2018**, 4, 1700429; c) Y. Zheng, G. J. N. Wang, J. Kang, M. Nikolka, H. C. Wu, H. Tran, S. Zhang, H. Yan, H. Chen, P. Y. Yuen, J. Mun, R. H. Dauskardt, I. McCulloch, J. B. H. Tok, X. Gu, Z. Bao, *Adv. Funct. Mater.* **2019**, 29, 1905340; d) M. Ashizawa, Y. Zheng, H. Tran, Z. Bao, *Prog. Polym. Sci.* **2020**, 100, 101181.
[111] H.-C. Hsieh, C.-C. Hung, K. Watanabe, J.-Y. Chen, Y.-C. Chiu, T. Isono, Y.-C. Chiang, R. R. Reghu, T. Satoh, W.-C. Chen, *Polym. Chem.* **2018**, 9, 3820.
[112] C. C. Jao, J. R. Chang, C. Y. Ya, W. C. Chen, C. J. Cho, J. H. Lin, Y. C. Chiu, Y. Zhou, C. C. Kuo, *Polym. Int.* **2020**, 70, 426.
[113] J. H. Kim, J. W. Park, *Sci. Adv.* **2021**, 7.
[114] H. M. Kim, Y. C. Kim, H. J. An, J.-M. Myoung, *J. Alloys Compd.* **2020**, 819, 153360.
[115] Y. Zhou, C. Zhao, J. Wang, Y. Li, C. Li, H. Zhu, S. Feng, S. Cao, D. Kong, *ACS Mater. Lett.* **2019**, 1, 511.
[116] K. Youssef, Y. Li, S. O'Keeffe, L. Li, Q. Pei, *Adv. Funct. Mater.* **2020**, 30, 1909102.
[117] H. Gao, S. Chen, J. Liang, Q. Pei, *ACS Appl. Mater. Interfaces* **2016**, 8, 32504.
[118] X. Yan, Z. Liu, Q. Zhang, J. Lopez, H. Wang, H.-C. Wu, S. Niu, H. Yan, S. Wang, T. Lei, J. Li, D. Qi, P. Huang, J. Huang, Y. Zhang, Y. Wang, G. Li, J. B. H. Tok, X. Chen, Z. Bao, *J. Am. Chem. Soc.* **2018**, 140, 5280.
[119] J. Liu, J. Wang, Z. Zhang, F. Molina-Lopez, G.-J. N. Wang, B. C. Schroeder, X. Yan, Y. Zeng, O. Zhao, H. Tran, T. Lei, Y. Lu, Y.-X. Wang, J. B. H. Tok, R. Dauskardt, J. W. Chung, Y. Yun, Z. Bao, *Nat. Commun.* **2020**, 11.
[120] H. L. Filiatrault, G. C. Porteous, R. S. Carmichael, G. J. Davidson, T. B. Carmichael, *Adv. Mater.* **2012**, 24, 2673.
[121] a) M. Bredol, H. Schulze Dieckhoff, *Materials* **2010**, 3, 1353; b) R. Withnall, J. Silver, P. G. Harris, T. G. Ireland, P. J. Marsh, *J. Soc. Inf. Disp* **2011**, 19, 798.
[122] J. S. Prener, F. E. Williams, *J. Electrochem. Soc.* **1956**, 103, 342.

[123] L. Wang, L. Xiao, H. Gu, H. Sun, *Adv. Opt. Mater.* **2019**, 7, 1801154.
[124] L. Cai, S. Zhang, Y. Zhang, J. Li, J. Miao, Q. Wang, Z. Yu, C. Wang, *Adv. Mater. Technol.* **2018**, 3, 1700232.
[125] W. A. D. M. Jayathilaka, A. Chinnappan, D. Ji, R. Ghosh, T. Q. Tran, S. Ramakrishna, *ACS Appl. Electron. Mater.* **2020**, 3, 267.
[126] H. Shin, B. K. Sharma, S. W. Lee, J. B. Lee, M. Choi, L. Hu, C. Park, J. H. Choi, T. W. Kim, J. H. Ahn, *ACS Appl. Mater. Interfaces* **2019**, 11, 14222.
[127] L. Shi, C. Zhang, Y. Du, H. Zhu, Q. Zhang, S. Zhu, *Adv. Funct. Mater.* **2020**, 31, 2007863.
[128] P. Xie, J. Mao, Y. Luo, *J. Mater. Chem. C* **2019**, 7, 484.
[129] Y. Zhou, S. Cao, J. Wang, H. Zhu, J. Wang, S. Yang, X. Wang, D. Kong, *ACS Appl. Mater. Interfaces* **2018**, 10, 44760.
[130] Y. Lee, J. W. Chung, G. H. Lee, H. Kang, J.-Y. Kim, C. Bae, H. Yoo, S. Jeong, H. Cho, S.-G. Kang, J. Y. Jung, D.-W. Lee, S. Gam, S. G. Hahm, Y. Kuzumoto, S. J. Kim, Z. Bao, Y. Hong, Y. Yun, S. Kim, *Sci. Adv.* **2021**, 7, eabg9180.

Table 1. Electroluminescent/mechanical performance of structure-enabled stretchable EL devices

Device category	Material and structure of EL unit[a)]	Maximum stretchability [%]	Stretch-release [cycles]	Turn-on voltage [V]	Maximum current efficiency [cd/A]	Maximum brightness [cd/m^2]	Ref.
Island-bridge LED	n-GaAs/AlInGaP/p-GaAs/	22	500 of 22% strain	-	-	-	[7]
	GaAs/$Al_{0.45}Ga_{0.55}As$/$In_{0.5}Al_{0.5}P$/$Al_{0.25}Ga_{0.25}In_{0.5}P$/$In_{0.56}Ga_{0.44}P$/$Al_{0.25}Ga_{0.25}In_{0.5}P$/$In_{0.5}Al_{0.5}P$/$Al_{0.45}Ga_{0.55}As$/GaAs	100	100,000 of 75% strain	-	-	-	[26b]
	-	20	1000 cycles of 20% strain	-	-	-	[36]
	White and RGB SMD LEDs (0402, Osram)	140, 250 in area	10000 cycles of 50% strain	-	-	-	[37]
Island-bridge OLED	ITO/TBADN:V_2O_5/TBADN/TCTA:TTPA/TBADN/TBADN:Liq/Al	30-50	-	~7	-	364	[26a]
	PDMS/silicone/SU-8/Al/MoO_3/NPB/Alq_3/LiF/Al/Ag/NPB	40	1000 of 40% strain	~2.5		~2000	[38]
	PDMS/PDMS pillars/SU-8/NPB/Al/LiF/Alq_3/NPB/MoO_3/Ag	35	1000 of 20% strain	4	3	~2000	[31]
	h-SEBS/s-SEBS/Au/IZO/GXR601/NDP9/BCFA/EML/NET-164/Liq/Al	30	1000 cycles of 25% strain	2.5	102	8510 @ 5 V	[131]
Buckling OLED	VHB/NOA63/Ag/MoO_3/NPB/mCP:Ir(ppy)$_3$/TPBi/Ca/Ag	80, 50 in area	100 of 25% in area	3	71	9699 @ 6.5 V	[51]
	VHB/NOA63/Ag/MoO_3/NPB/mCP:Ir(ppy)$_3$/TPBi/Ca/Ag	100	15000 of 100% strain	3	70	~11000 @ 7 V	[49]
	VHB/NOA63/Ag/MoO_3/NPB/CBP:Ir(BT)$_2$(acac)/TPBi/Ca/Ag	100	20000 of 20% strain	-	73	-	[48]
	VHB/NOA63/Ag/MoO_3/NPB/mCP:Ir(ppy)$_3$/TPBi/Ca/Ag	100	35000 of 20% strain	-	66	15110	[50]
Buckling PLED	PDMS/PET/PEDOT:PSS/PPE-PPV/LiF/Al	100	-	<5	0.026	113 @ 9 V	[42]
	Ecoflex/parylene/polyimide/ITO/HTL/EML/NaF/Al/SiON/parylene	200	1000 of 60% strain	-	-	4900	[43]
	PDMS/PEDOT:PSS/PDY-132/PEI/ZnO/Al	20	1000 of 10% biaxial strain	2.4	7.76	8000	[52]
Buckling QLED	PDMS/PEN/Graphene/PEDOT:PSS/TFB/CdSe-	70	100 of 70% strain	2.8	2.25	1310	[47]

	CdS-ZnS QDs/TiO_2/Al/Ecoflex						
	VHB/parylene/SU-8/ITO/PEDOT:PSS/TFB/ CdSe-ZnS QDs/ZnO/Al/ITO/SU-8/parylene	50	-	3	17.52	43000 @ 9V	[65]
	VHB/PI-AgNWs/PEDOT:PSS/TAPC:PVA/$CH_3NH_3PbBr_3$ QDs/TPBi/CsF/Al	50	1000 of 20% strain	3.2	9.2	3187 @ 9 V	[19]
Textile OLED	PET/ITO/HAT-CN/TAPC/TCTA:Ir(ppy)$_2$ acac/B3PYMPM/Liq/Al	20	-	2.3	46	4300	[56]
Textile ACEL	TPU-$[EMIM]^+[TFSI]^-$ /ZnS-PU/Ag/nylon	-	1000	-	-	115.1	[57]
	nylon-spandex/Au/ZnS:Cu-Ecoflex/Au/nylon-spandex	200	1000 cycles of 50% strain	-	-	-	[55]
Kirigami OLED	-	5	-			300	[40b]

[a] Abbreviations: AgNWs, silver nanowires; CNTs, carbon nanotubes; TBADN, 3-tert-butyl-9,10-di(2-naphthyl)anthracene; TCTA, 4,4',4",-tri(N-carbazolyl)triphenylamine; TTPA, 9,10-bis[N,N-di-(p-tolyl)-amino]anthracene; Liq, 8-Hydroxyquinolinolato-lithium; ITO, indium tin oxide; PDMS, polydimethylsiloxane; Alq_3, Tris(8-hydroxyquinoline)aluminum; NPB, N,N′-bis(naphthalen-1-yl)-N,N′-bis(phenyl)-benzidine; MoO_3, molybdenum oxide; $Ir(ppy)_3$, tris(2-phenylpyridine)iridium; mCP, N,N′-dicarbazolyl-3,5-benzene; h-SEBS, hard styrene-ethylene-butylene-styrene; s-SEBS, soft styrene-ethylene-butylene-styrene; IZO, indium zinc oxide; BCFA, N-([1,1′-biphenyl]-4-yl)-9,9-dimethyl-N-(4-(9-phenyl-9H-carbazol-3-yl)phenyl)-9H-fluoren-2-amine; TPBi, 1,3,5-tris(Nphenyl-ben-zimidazol-2-yl)benzene; CBP, (4,4′-bis (N-carbazolyl)-1, 1′-biphenyl); $Ir(BT)_2(acac)$, (2,3,5,6-tetrakis(3,6-diphenylcarbazol-9-yl)-1,4-dicyanobenzene); PET, polyethylene terephthalate; PEDOT:PSS, poly(3,4 ethylenedioxythiophene):poly (styrenesulphonate); PPE-PPV, poly(p-phenylene-ethynylene)-altpoly(p-phenylene-vinylene); HTL, hole transporting layer; EML, emissive layer. PEI, polyethylenimine; PEN, polyethylene naphthalate; TFB, Poly[(9,9-dioctylfluorenyl-2,7-diyl)-co-(4,4′-(N-(4-s-butylphenyl))diphenylamine)]; QDs, quantum dots; TAPC, 4,4'-cyclohexylidenebis[N,N-bis(4-methylphenyl)benzenamine]; PVA, poly(vinyl alcohol); TPBi, 2,2',2"-(1,3,5-Benzinetriyl)-tris(1-phenyl-1-H-benzimidazole); HAT-CN, 1,4,5,8,9,11-hexaazatriphenylenehexacarbonitrile; $Ir(ppy)_2acac$, bis[2-(2-pyridinyl-N)phenyl-C](acetylacetonato)iridium; B3PYMPM, 4,6-Bis(3,5-di(pyridin-3-yl)phenyl)-2-methylpyrimidine, 4,6-Bis(3,5-di-3-pyridinylphenyl)-2-methylpyrimidine; TPU, thermoplastic polyurethane; $[EMIM]^+[TFSI]^-$, 1-ethyl-3-methylimidazolium:bis(trifluoromethylsulfoyl) imide; PU, polyurethane; MADN, 2-methyl-9,10-di(2-naphthyl) anthracene; Pyrene-CN, 1,6-bis(N-phenyl-p-CN-phenylamino)-pyrenes.

Table 2. Conductivity, transmittance, and stretchability of intrinsically stretchable TCEs

Electrode type	Materials [a)]	Conductivity and sheet resistance	Maximum strain[%]	Stretch release [cycles]	Transmittance[%]	Surface roughness	Ref
Ionically conductive transparent electrode	PVA-PEO-LiCl	0.055 S/cm	1000	-	~70	-	[80]
	PAM-LiCl	3.2 S/cm	400	-	93	-	[54]
	PAM-LiCl	-	-	-	-	-	[76]
	PAM-LiCl	-	>487	10 cycles of 400% strain	-	-	[67a]
	PAM-LiCl	-	>325	-	-	-	[67b]
	PVA-PEO-KOH	0.29 S/cm	800	1000 cycles of 300% strain	92	-	[78]
	P(VDF-HFP)-EMITFSI	-	>1000	-	94	-	[79]
	$LiClO_4$-PC-PMMA	-	700	1000 cycles of 700 % strain	~ 100%	-	[72]
Conductive thin layer on surface of elastomer	PEDOT:PSS-PEO/PDMS	140 Ω/sq	40	-	82	-	[88]
	PU/PEDOT:PSS	-	-	-	-	-	[112]
	Au/PDMS	-	~20-30	-	26% at 630 nm	Rq = 4.54 nm	[120]
	PDMS/AgNWs	-	-	-	-	-	[59a]
	Au/nylon and Au/spandex	3.6±0.9 Ω/sq	200% strain with R/R0 < 2	1000 cycles of 50 % strain	<40, increase to 58% under 120% strain	-	[55]
	AgNWs/PDMS	-	-	-	-	120 nm	[90]
	AgNWs/PDMS	-	-	-	-	-	[23]
	AgNWs-PUU/PDMS	3 Ω/sq	>150	5000 cycles of 100% strain	70.1	-	[91]
	AgNWs/PDMS	-	-	-	-	-	[124]
	AgNWs/TPU	2.1 Ω/sq	100	1000 cycles of 50% strain	39.6	-	[129]
	silicon/CNT-silicon	0.47 kΩ/cm	200	1000 cycles of 200 % strain	-	-	[59b]
	Au/PDMS	3.6 Ω/sq	95	200 cycles of 40% strain	reflective	Rq= 5.0±0.8	[64a]

	H-SEBS/AgNWs	-	-	-	-	-	[115]
	Graphene/AgNWs-PEDOT:PSS/Graphene/PDMS	58 Ω/sq	85	50 cycles of 80 % strain	78	Rmax = 10 nm	[126]
	AgNWs/PDMS	26.8 Ω/sq	180	5000 cycles of 50% strain	91.8	-	[70b]
	PEDBU-AgNWs/PDMS	5-8 Ω/sq	120	10000 cycles of 50% strain	-	-	[95a]
Conductive network Embedded in elastomer	AgNWs-GO/PUA	14 Ω/sq	100	100 cycles of 0-40% strain	88	peak to valley 10 nm	[92b]
	PDMS/aerogel/AgNWs	-	-	-	-	-	[113]
	PDMS/aerogel/AgNWs	15 Ω/sq	70	100 cycles of 0-25% strain	80	-	[104]
	SWCNT/PtBA	500 Ω/sq	50	14 cycles of 0-40% strain	87	average surface roughness <10 nm	[61]
	AgNWs/PUA	15 Ω/sq	120	1500 cycles of 0-30% strain	83	peak to valley 3.4 nm	[92a]
	AgNWs/PUA	-	-	-	-	-	[119]
	PDMS–$MPU_{0.4}$–$IU_{0.6}$/CNT	-	50	-	-	-	[10b]
	CNT/PU	-	450	350 cycles of 200% strain	<40		[68]
	AgNWs/CF/PDMS	15 Ω/sq	70	200 cycles of 30% strain	85	Rq ~22 nm	[92c]
	AgNWs/PDMS	7.3 Ω/sq	80	-	79.6	Ra = 18 nm	[92d]
	AgNWs/SEBS	18 Ω/sq	100, 40 times increase	1000 cycles of 50 % strain	88	-	[77]
	Chitosan/EA/AgNWs	8.4 Ω/sq	130	100 cycles of 30 % strain	89	-	[75]

[a)]Abbreviation: AgNWs, silver nanowires; SWCNTs, single wall carbon nanotubes; PVA, poly(vinyl alcohol); PEO, polyethylene glycol; PAM, polyacrylamide; (P(VDF-HFP) fluoroelastomer poly(vinylidene fluoride-co-hexafluoropropene); EMITFSI, 1-ethyl-3-methylimidazolium bis(trifluoromethylsulfonyl) imide; $LiClO_4$, lithium percolate; PC, propylene carbonate; PMMA, poly(methyl methacrylate); PEDOT:PSS, poly(3,4 ethylenedioxythiophene):poly (styrenesulphonate); PU, polyurethane; PDMS, polydimethylsiloxane; PUU, polyurethane urea; TPU, thermoplastic polyurethane; H-SEBS, hydrogenated styrenic thermoplastic elastomer; PEDUB, polyurethane equipped with dynamic

urea bonds; GO, graphene oxide; PtBA, poly(tert-butyl acrylate); PUA, polyurethane acrylate; MPU, 4,4'-methylenebis(phenyl urea) unit; IU, isophorone bisurea unit; CF, Clear Flex 50; SEBS, styrene-ethylene-butylene-styrene; EA, ethanolamine.

Table 3. Electroluminescent/mechanical performance of material-enabled stretchable EL devices

Device category	Material and structure [a)]	Maximum stretchability [%]	Stretch release [cycles]	Turn-on voltage [V]	Maximum current efficiency [cd/A]	Maximum brightness [cd/m^2]	Driving conditions (ACEL devices)	Ref.
ACEL device	TPU+Ag/ZnS:Cu+DS/ PVA-PEO-LiCl	450	-	-	-	59.6	4.21 V/μm, 3k Hz	[80]
	Spandex fabric/Pyy/ZnS-silicone/LiCl-PAM	100	100 of 100 % strain	-	-	70	5 V/μm, 2k Hz	[54]
	PAM-LiCl/VHB/ZnS/VHB/LiCl-PAM	1500 in area	-	-	-	9.4	3.6 kV, 1k Hz	[76]
	Ecoflex/PAM-LiCl/Ecoflex-ZnS/PAM-LiCl/Ecoflex	487	-	-	-	-	25 kV/cm, 700 Hz	[67a]
	Ecoflex/PAM-LiCl/Ecoflex-ZnS/PAM-LiCl/Ecoflex	325, 200 in area	-	-	-	<30	2.5 kV/cm, 700 Hz	[67b]
	PVA-PEO-KOH/ZnS-silicone/PVA-PEO-KOH	800	1000 of 300% strain	-	-	233.4	7.7 V/μm, 2.5 kHz	[78]
	P(VDF-HFP)-EMITFSI/P(VDF-HFP)-FS300-ZnS/P(VDF-HFP)-EMITFSI	800	1000 of 20 % strain	23	-	1460	3750 V, 50 Hz	[79]
	VHB/$LiClO_4$+PC+PMMA/ZnS:Cu+Ecoflex/$LiClO_4$+PC+PMMA/VHB	700	1000 of 400% strain	-	-	95	4.5 V/μm, 2k Hz	[72]
	PDMS/AgNWs/PDMS-ZnS/AgNWs	80	6000 of 50 % strain	-	-	307.3	500 V, 5k Hz	[59a]
	PDMS/AgNWs/ZnS:Cu-PDMS/AgNWs/PDMS	100	1000 of 80% strain	60	-	~40	±120 V, 2.5k Hz	[90]
	PDMS/AgNWs/$BaTiO_3$+ZnS:Cu+PDMS/AgNWs/PDMS	110	500 of 50% strain	-	-	121	250 V, 2.2 kHz	[23]
	PDMS/AgNWs/PUU-ZnS/AgNWs/PDMS	150	5000 for 100% strain	-	-	~100	300 V, 500 Hz	[91]
	AgNWs/PDMS-ZnS/AgNWs	20	1000 of 20 % strain	-	-	~300	2000 V, 500 Hz	[124]
	TPU/AgNWs/e-PVDF-HFP-ZnS/AgNWs/TPU	100, 47 in area	500 of 50 % strain	-	-	785	180 V, 20k Hz	[129]
	silicon/CNT/silicon/ZnS-silicon/CNT	200	200 of 200% strain	-	-	12.66	6 V/μm, 1.5 kHz,	[59b]

	PDMS/Au/PDMS-ZnS/PEDOT:PSS-Triton X-100	40	-	-	-	-	165 V, 37k Hz	[64a]
	H-SEBS/AgNWs/BT+PVP-PVDF-HFP+ZnS:Cu/AgNWs/H-SEBS	50	500 of 50 % strain	-	-	~310	60 V, 17kHz	[115]
	PDMS/H-GrPGr/PDMS-ZnS:Mn/H-GrPGr/PDMS	80	-	-	-	~100	4 V/μm, 10k Hz	[126]
	PDMS/AgNWs/PDMS-ZnS/AgNWs/PDMS	50	5000 of 50% strain	-	-	82	3.5 V/μm, 10k Hz	[70b]
	PDMS/AgNWs-PEDUB/PEDUB-ZnS/PEDUB-AgNWs/PDMS	140	5000 of 100% strain	-	-	82.4	300 V, 500 Hz	[95a]
	PDMS–$MPU_{0.4}$–$IU_{0.6}$/CNT/PDMS–$MPU_{0.4}$–$IU_{0.6}$-ZnS:Cu/CNT/PDMS–$MPU_{0.4}$–$IU_{0.6}$	250	100 of 50% strain	-	-	-	150 V, 300 Hz	[10b]
	PU/CNT/PU-ZnS/CNT/PU	400	350 of 200 % strain	-	-	121.2	15 V/μm, 2.6k Hz	[68]
	PDMS/CF/AgNWs/PDMS-ZnS:Cu/AgNWs/CF/PDMS	60	-	-	-	-	-	[92c]
	PDMS/AgNWs/PDMS-ZnS/AgNWs/PDMS	70	-	-	-	25.7	130 V, 800 Hz	[92d]
	SEBS/AgNWs/ZnS-PVDF-HFP-$BaTiO_3$/AgNWs/SEBS	100	500 of 50% strain	12	-	115	50 V, 12kHz	[77]
	Chitosan/EA/AgNWs/PVDF/ZnS:Cu-PDMS/AgNWs	100	-	-	-	~70	450 V, 500Hz	[75]
Perovskite-polymer LED	PDMS/PEDOT:PSS/$CH_3NH_3PbBr_3$-PEO/EInGa	40	100 of 40% strain	2.4	3.2	15960 @ 8.5 V	-	[88]
PLEC	PDMS/Au/PDMS-Ru(dtb-bpy)$_3$$(PF6)_2$/EGaIn	27	50 of 15% strain	-	-	work @ 5V	-	[120]
	SWCNT-PtBA/(PF-B)-(PEO-DMA)-LiTf/SWCNT-PtBA	45	-	4.8	1.16	200 @ 11 V	-	[61]
	AgNWs-PUA/PEDOT:PSS/SuperYellow-PEO-ETPTA-LiTf/AgNWs-PUA	120	1000 of 30 % strain	6.8	11.4	2200 @ 21 V	-	[92a]
	PUA/AgNWs/PEDOT:PSS/SuperYellow+ion-conducting polymer+ETT-15+LiTf/AgNWs/PUA	30	20 of 30% strain	-	-	-	-	[119]

PLED	PU/PEDOT:PSS/PF-b-PI/EInGa	140	100 of 50% strain	-	-	70 @ 10 V	-	[112]
	AgNWs-GO/PUA/PEDOT:PSS /white light emitting polymer-OXD-7/PEI/AgNWs-GO/PUA	130	100 of 40% strain	7	4	1100 @ 21 V	-	[92b]
	PDMS/aerogel/AgNWs/PEDOT:PSS-Triton X/SuperYellow-Triton X/ZnO/d-PEIE/AgNWs/ZnO/d-PEIE	80	200 of 40% strain	8.3	1.6	4400 @ 11 V	-	[113]

[a)]Abbreviation: AgNWs, silver nanowires; SWCNTs, single wall carbon nanotubes; PVA, poly(vinyl alcohol); DS, dragon skin; PEO, polyethylene glycol; PAM, polyacrylamide; PPy, polypyrrole; (P(VDF-HFP) fluoroelastomer poly(vinylidene fluoride-co-hexafluoropropene); EMITFSI, 1-ethyl-3-methylimidazolium bis(trifluoromethylsulfonyl) imide; $LiClO_4$, lithium percolate; PC, propylene carbonate; PMMA, poly(methyl methacrylate); PEDOT:PSS, poly(3,4 ethylenedioxythiophene):poly (styrenesulphonate); BT, barium titanate; PVP, poly(vinyl pyrrolidone); PU, polyurethane; H-GrPGr, bilayer graphene/PEDOT:PSS/bilayer graphene; PDMS, polydimethylsiloxane; Triton X-100, t-octylphenoxypolyethoxyethanol; PUU, polyurethane urea; TPU, thermoplastic polyurethane; H-SEBS, hydrogenated styrenic thermoplastic elastomer; PEDUB, polyurethane equipped with dynamic urea bonds; GO, graphene oxide; PtBA, poly(tert-butyl acrylate); PUA, polyurethane acrylate; MPU, 4,4'-methylenebis(phenyl urea) unit; IU, isophorone bisurea unit; CF, Clear Flex 50; SEBS, styrene-ethylene-butylene-styrene; EA, ethanolamine; EGaln, eutectic indium-gallium alloy; $Ru(dtb\text{-}bpy)_3^{2+}(PF_6)^-_2$, Tris(4,4'-di-tert-butyl-2,2'-bipyridine)ruthenium bis(hexafluorophosphate); PF-B, blue emissive polyfluorene copolymer; PEO-DMA, (poly(ethylene oxide) dimethacrylate ether; LiTf, lithium trifluoromethane sulfonate; ETT-15, ethoxylated trimethylopropane triacrylate; PF-b-PI, poly[2,7-(9,9-dioctylfluorene)]-block-poly(isoprene); OXD-7, 1,3-bis[(4-tert-butylphenyl)-1,3,4-oxidiazolyl]phenylene; d-PEIE, doped polyethylenimine, ethoxylated;

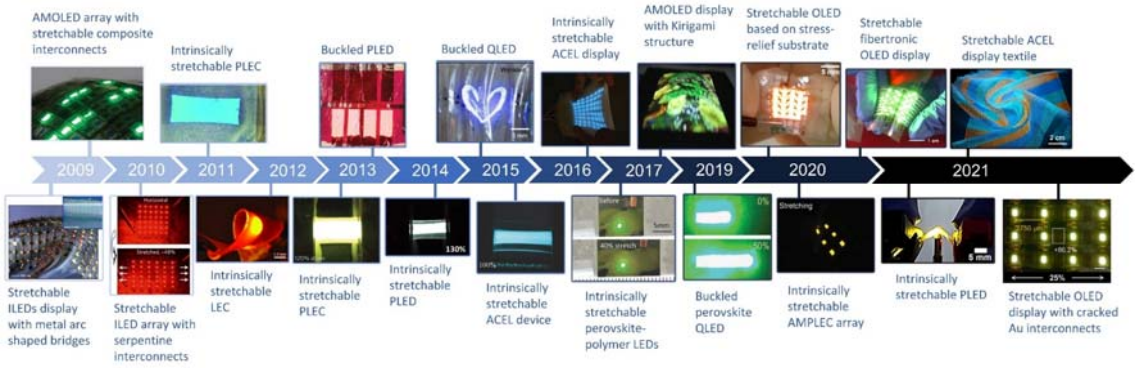

Figure 1. Timeline of the development of stretchable EL devices. Stretchable ILEDs display with metal arc shaped bridges (2009): Reproduced with permission.[7] Copyright 2009, AAAS. AMOLED array with stretchable composite interconnects (2009): Reproduced with permission.[26a] Copyright 2009, Nature Publishing Group. Stretchable ILED array with serpentine interconnects (2010): Reproduced with permission.[26b] Copyright 2010, Nature Publishing Group. Intrinsically stretchable PLEC (2011): Reproduced with permission.[61] Copyright 2011, Wiley-VCH. Intrinsically stretchable LEC (2012): Reproduced with permission.[120] Copyright 2012, Wiley-VCH. Intrinsically stretchable PLEC (2013): Reproduced with permission.[92a] Copyright 2013, Nature Publishing Group. Buckled PLED (2013): Reproduced with permission.[42] Copyright 2013, Nature Publishing Group. Intrinsically stretchable PLED (2014): Reproduced with permission.[92b] Copyright 2014, American Chemical Society. Buckled QLED (2015): Reproduced with permission.[44] Copyright 2015, Nature Publishing Group. Intrinsically stretchable ACEL device (2015): Reproduced with permission.[90] Copyright 2015, Wiley-VCH. Intrinsically stretchable ACEL display (2016): Reproduced with permission.[67a] Copyright 2016, AAAS. Intrinsically stretchable perovskite-polymer LEDs (2017): Reproduced with permission.[88] Copyright 2017, Wiley-VCH. AMOLED display with stretchable openings (2017): Reproduced with permission.[40b] Copyright 2017, Society for Information Display. Buckled perovskite QLED (2019): Reproduced with permission.[19] Copyright 2019, Wiley-VCH. Stretchable OLED based on stress-relief substrate (2020): Reproduced with permission.[31] Copyright 2020, American Chemical Society. Intrinsically stretchable AMPLEC array (2020): Reproduced with permission.[119] Copyright 2020, Nature Publishing Group. Stretchable fibertronic OLED display (2020): Reproduced with permission.[56] Copyright 2020, American Chemical Society. Intrinsically stretchable PLED (2021): Reproduced with permission.[113] Copyright 2021, AAAS. Stretchable ACEL display textile (2021): Reproduced with permission.[57] Copyright 2021, Nature Publishing Group. Stretchable OLED display with cracked Au interconnects (2021): Reproduced with permission.[130] Copyright 2021, AAAS.

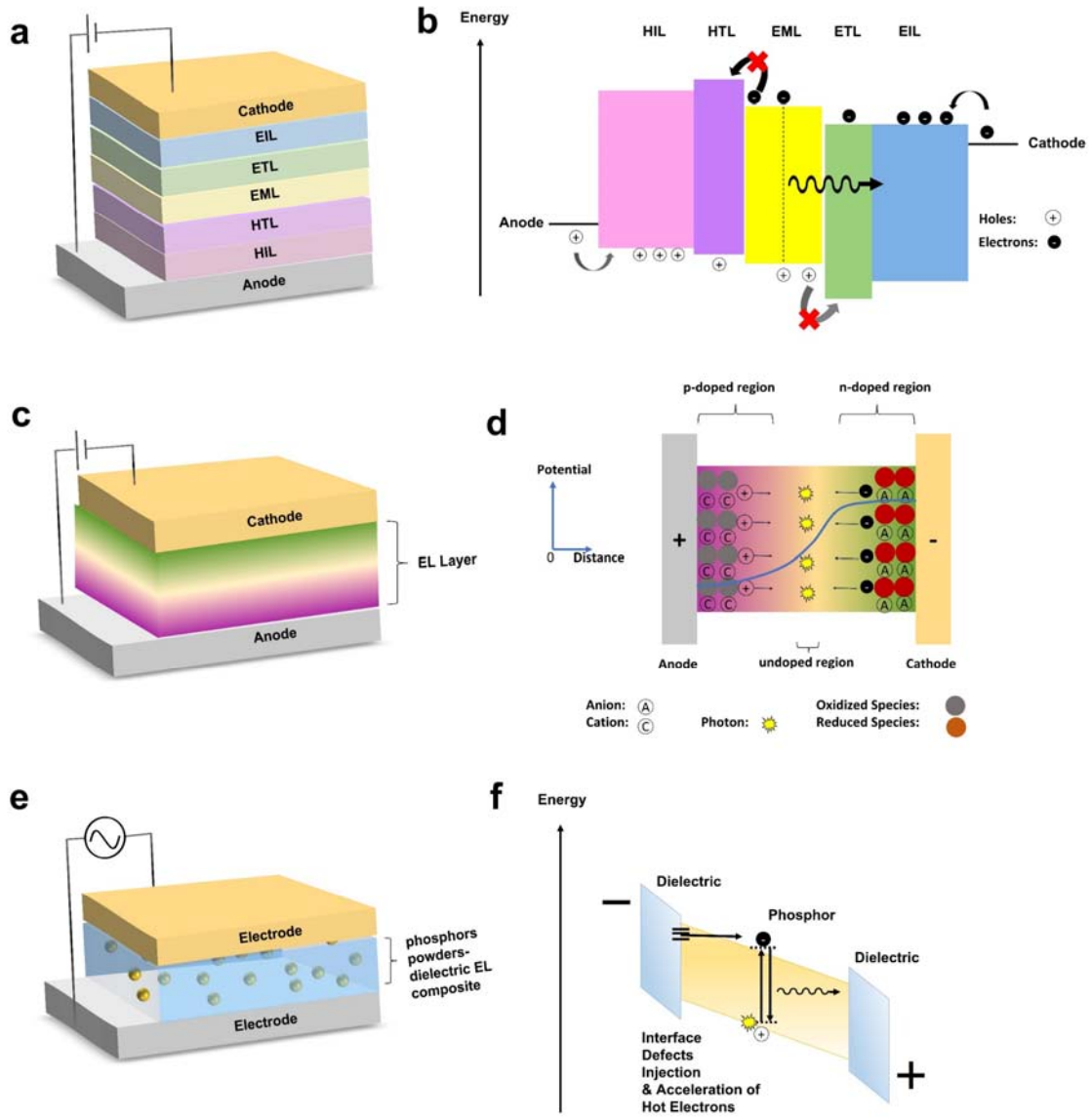

Figure 2. Device structures of a) OLED, c) LEC, and e) ACEL device. Schematic illustration of the energy diagrams photo generation in b) OLED, d) LEC, and f) ACEL device.

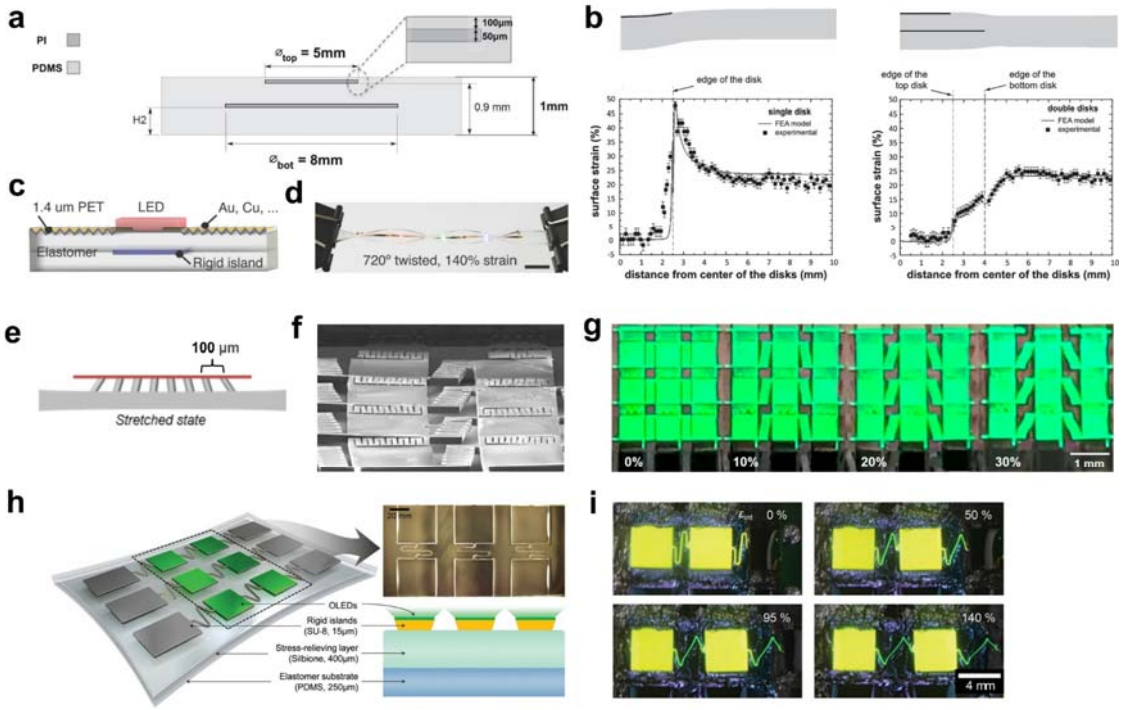

Figure 3. Structure-enabled stretchable EL devices of island-bridge structures. a) Schematic of a dual-disk structure of polyimide thin coupons in PDMS. b) FEA analysis of strain profile of a single-disk structure and the dual-disk structure. Reproduced with permission.[36] Copyright 2014, American Institute of Physics. c) Scheme of polyimide-assisted strain-insulated island, where an LED unit is mounted on top of polyimide embedded area. d) Photograph of the LED strip being twisted at 720° and stretched at 140% strain. Reproduced with permission.[37] Copyright 2015, Wiley-VCH. e) Schematic of cross section of PDMS pillars between SU-8 rigid island and PDMS substrate. f) SEM image of SU-8 islands and interconnects. g) Photograph of stretchable OLED being stretched from 0 to 30%. Reproduced with permission.[31] Copyright 2020, American Chemical Society. h) Schematic illustration of stretchable OLED achieved by introducing ultrasoft Silbione layer between SU-8 and PDMS substrate. i) Photograph of stretchable OLED where 140% maximum stretchability for the interconnects was demonstrated. Reproduced with permission.[38] Copyright 2020, Wiley-VCH.

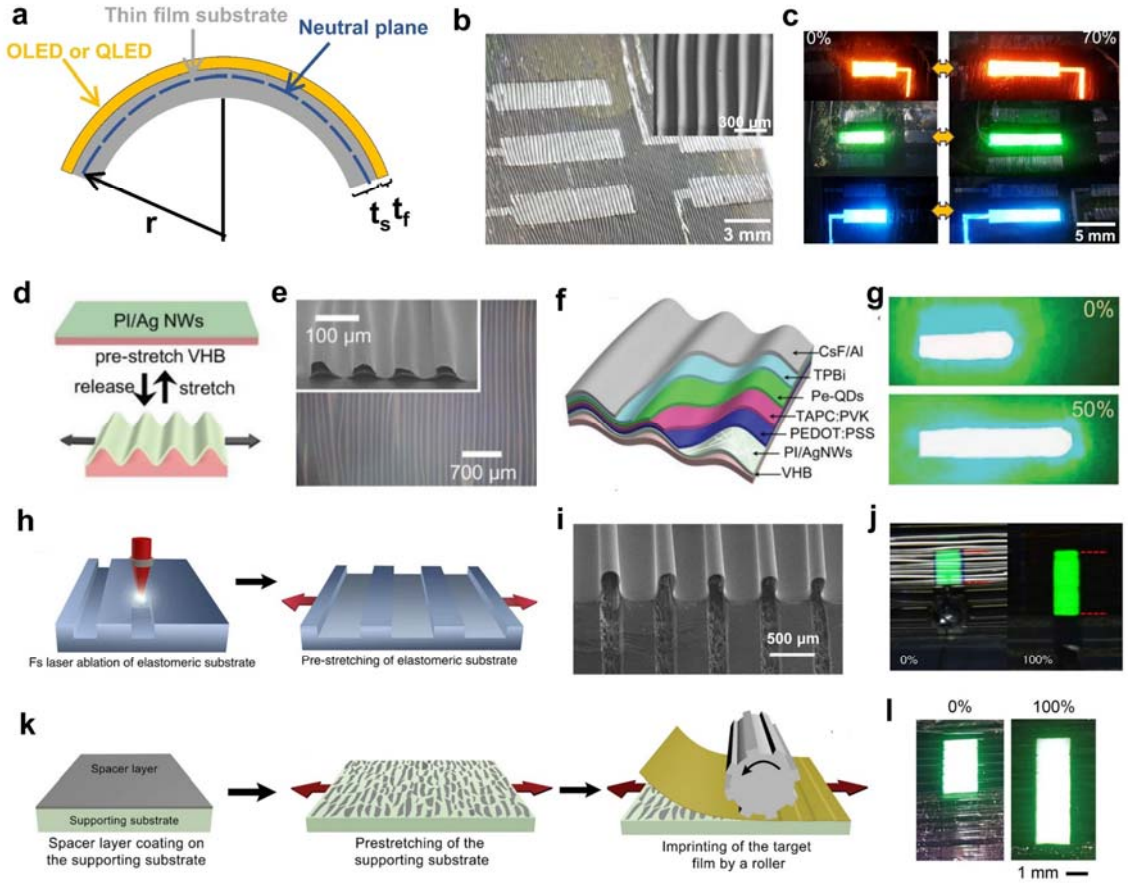

Figure 4. Structure-enabled stretchable EL devices of buckling structures. a) Schematic illustrations for calculating bending strain of OLEDs or QLEDs on ultrathin film substrate. b) Image of buckled wavy QLED on pre-stretched Ecoflex substrate. SEM image of the wavy structure in inset. c) Photograph of red, green, and blue QLEDs stretched from 0 to 70% strain. Reproduced with permission.[47] Copyright 2017, American Chemical Society. d) Schematic of transferring AgNWs/Polyimide to pre-stretched VHB. e) SEM image of surface morphology of AgNWs/polyimide wrinkles on VHB substrate. f) Schematic of QLEDs structure. g) Optic image of the stretchable QLED at 0 and 50% strain in on state. Reproduced with permission.[19] Copyright 2019, Wiley-VCH. h) Schematic of creating period groove on elastomer surface via laser ablation. i) SEM image of periodic wrinkles formed on the grooves. j) Photograph of 200% pre-strained stretchable OLED being stretched from 0 to 100% strain. Reproduced with permission.[49] Copyright 2016, Nature Publishing Group. k) Schematic illustration of creating selective adhesion between OLED thin film and elastomer substrate via spacing layer and patterned roller. l) Photograph of the stretchable OLED being stretched from 0 to 100% strain. Reproduced with permission.[50] Copyright 2019, Wiley-VCH.

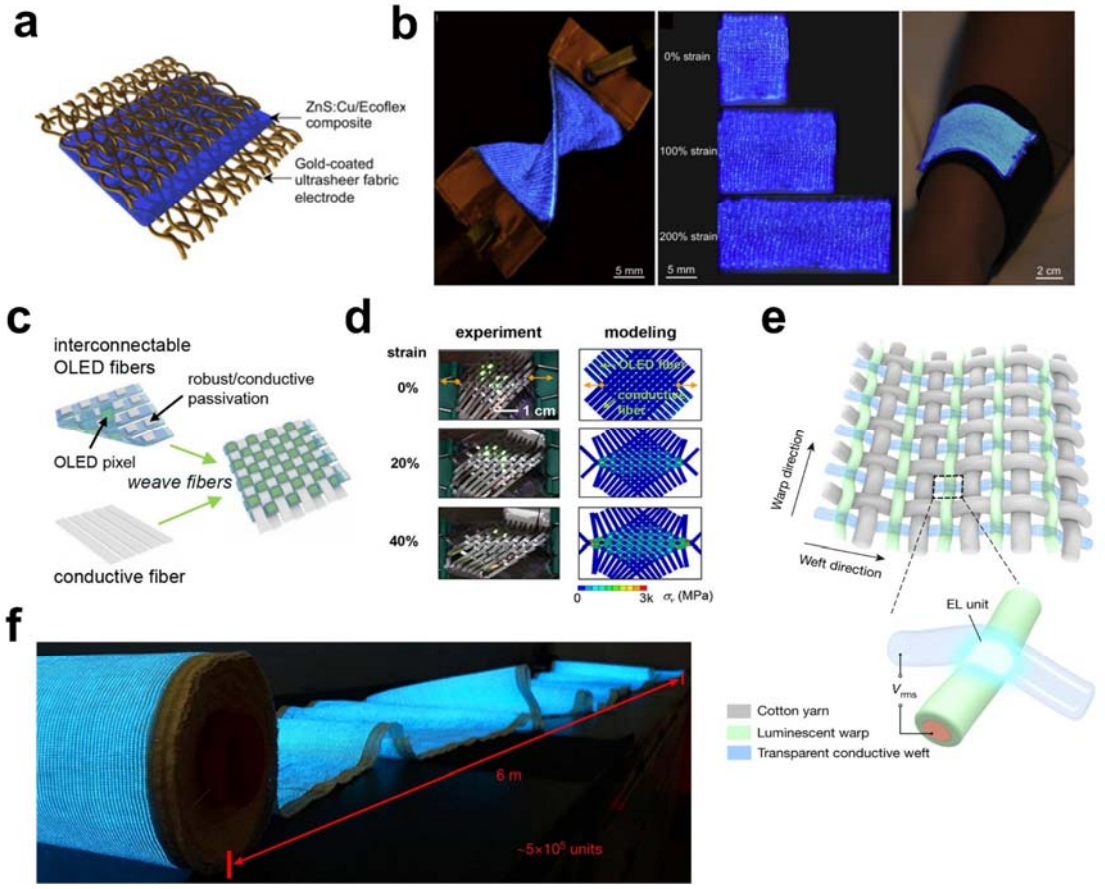

Figure 5. Structure-enabled stretchable EL devices of textile structures. a) Diagram of the ACEL device structure where gold coated ultrasheer fabrics were employed as electrodes sandwiching ZnS:Cu-Ecoflex EL composite. b) Photographs of the device being twisted, stretched, and bended. Reproduced with permission.[55] Copyright 2020, Elsevier. c) Schematic illustration of the fabrication process of fibertronic OLEDs. d) Photographs and modelling result of the device being stretched along the diagonals of weaved openings. Reproduced with permission.[56] Copyright 2020, American Chemical Society. e) Schematic of the weave structure of the display textile. EL units form at the interlace between contacting luminescent warp and transparent conductive weft. f) Photograph of a 6-m-long display textile consisting of approximately 5 × 10^5 EL units. Reproduced with permission.[57] Copyright 2021, Nature Publishing Group.

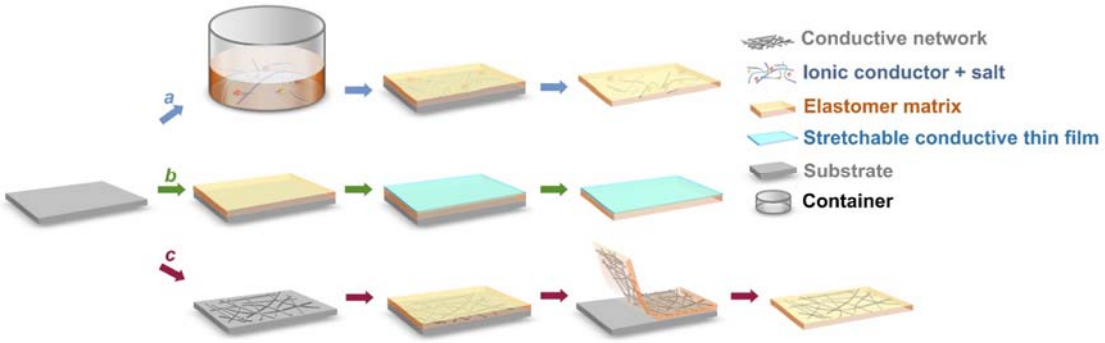

Figure 6. Schematic illustration of the fabrication process of three typically stretchable TCEs applied in intrinsically stretchable EL devices. a) Ionically conductive transparent electrode. b) Transparent conductive thin layer coated on elastomer substrate. c) Transparent conductive network embedded in elastomer surface.

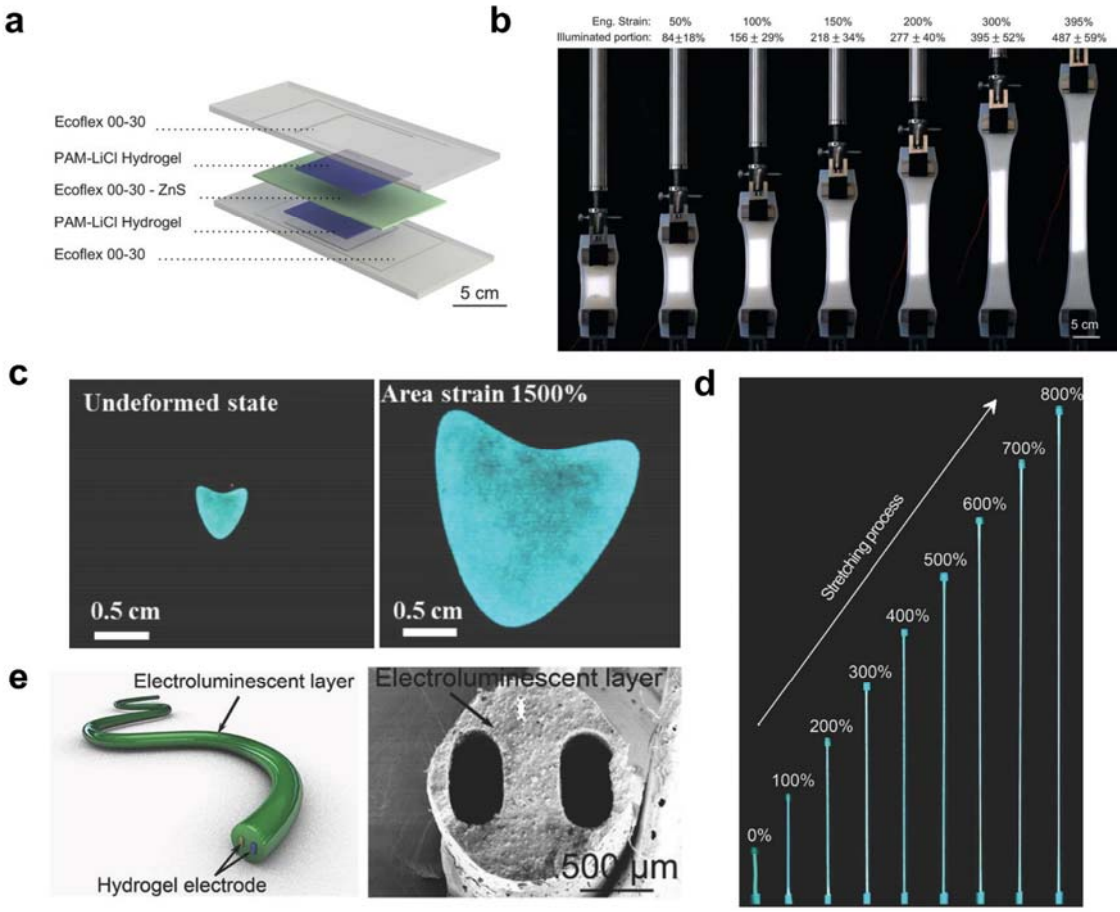

Figure 7. Ionically conductive transparent electrodes for intrinsically stretchable ACEL devices. a) Scheme of five-layers-structure of the stretchable ACEL devices. b) Photograph of the luminescent behavior of devices under uniaxial test. The strain of Illuminated portion was calculated based on engineering strain (grip to grip). The device was driven in electric field ~25 kV/cm. Reproduced with permission.[67a] Copyright 2016, AAAS. c) Photograph of the EL performance of the stretchable ACEL device at relaxed state (left) and 1500% area strain (right). The device was biased at cyclic voltage of 5 kV and 1k Hz. Reproduced with permission.[76] Copyright 2016, Wiley-VCH. d) Photograph of the ACEL fiber being stretched up to 800% strain. e) Schematic illustration of co-extruded ACEL fiber (left). SEM image of the cross-section of the ACEL fiber (right). Reproduced with permission.[78] Copyright 2018, Wiley-VCH.

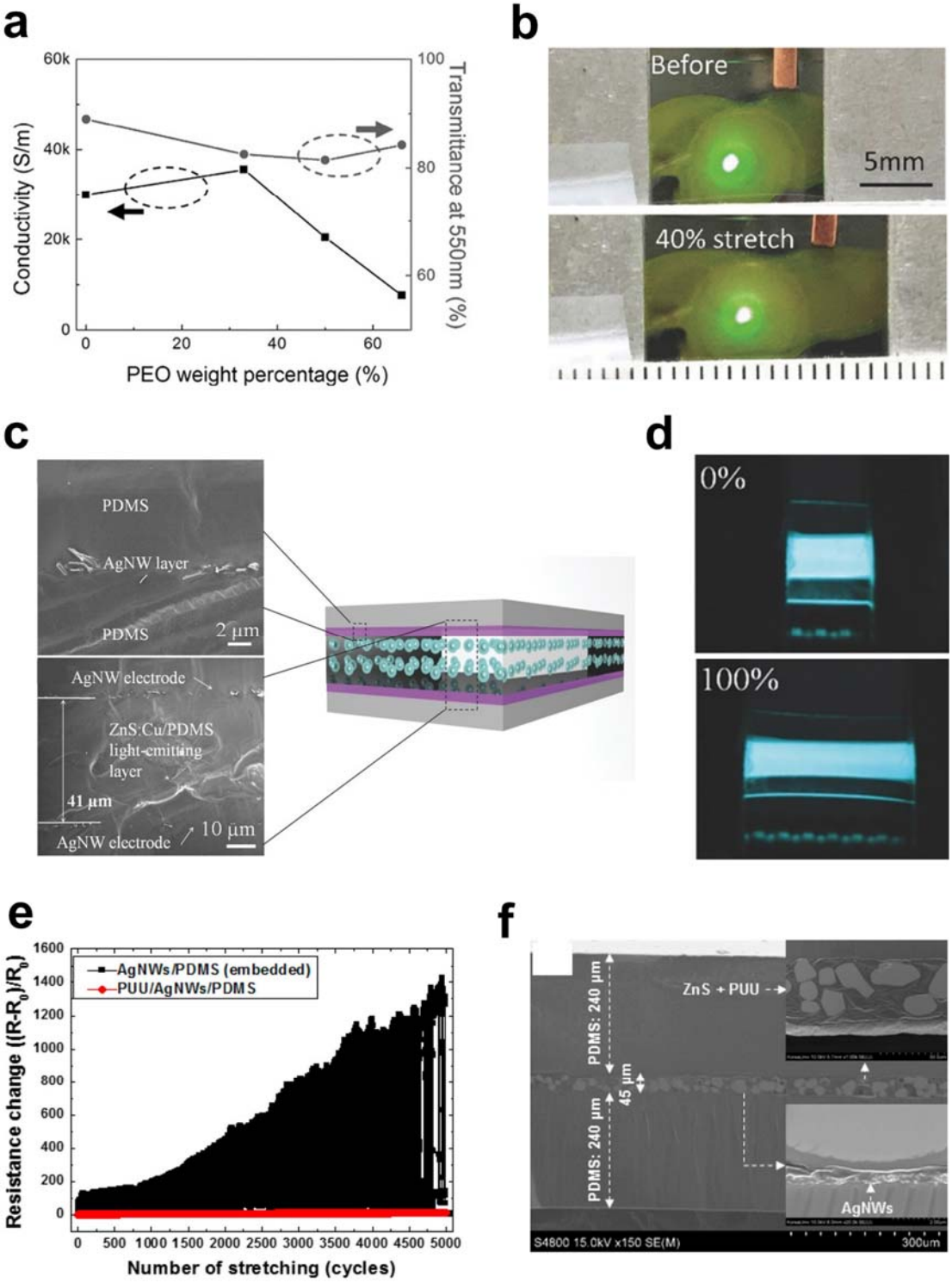

Figure 8. Transparent conductive thin layer coated on elastomer substrate for intrinsically stretchable EL devices. a) Figure of conductivity and transmittance vs weight percentage of PEO in PEDOT:PSS-PEO electrode. Peak conductivity was observed at 33 wt% PEO. b) Photographs of perovskite-PEO LED before

and after 40%. The LED was biased at 4 V. Reproduced with permission.[88] Copyright 2017, Wiley-VCH. c) Schematic illustration of the ACEL device structure where two AgNWs/PDMS electrodes sandwiched ZnS:Cu/PDMS EL layer. d) Photographs of the ACEL device being stretched from 0 to 100% strain. Reproduced with permission.[90] Copyright 2015, Wiley-VCH. e) Figure of stretch-release cycling test applied on AgNWs/PDMS (embedded structure) and PUU coated AgNWs/PDMS electrode. f) SEM image of the cross-section of the ACEL device. Reproduced with permission.[91] Copyright 2017, American Chemical Society.

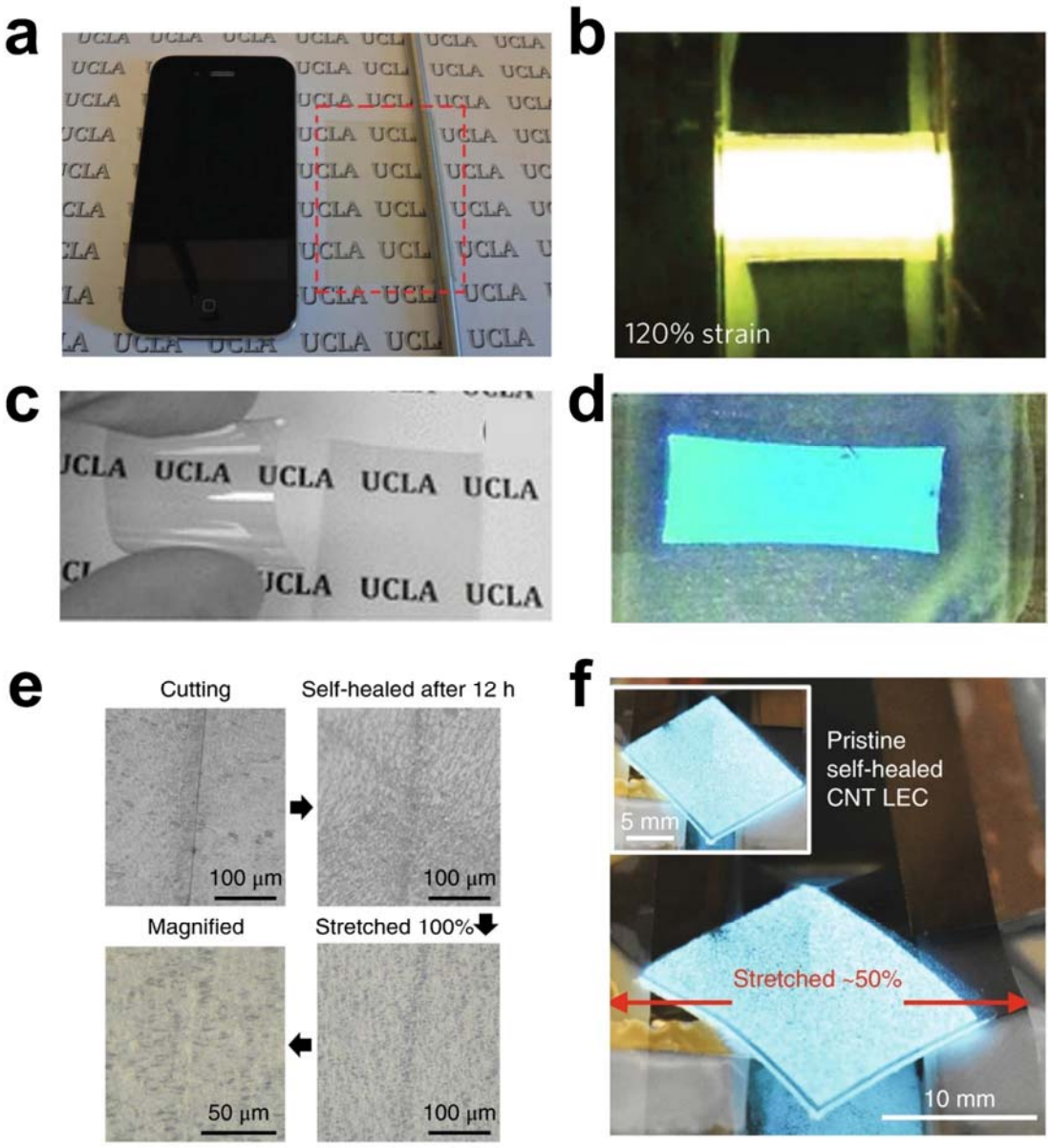

Figure 9. Transparent conductive network embedded in elastomer surface for intrinsically stretchable EL devices. a) Optic photograph of a AgNWs/PUA film with sheet resistance of 15 Ω/sq partially rolled on a rod. b Photograph of the PLEC being stretched to 120% strain. Reproduced with permission.[92a] Copyright 2013, Nature Publishing Group. c) Photograph of transparent CNTs/PtBA electrode. d) Photograph of the PLEC being stretched to 45%. Reproduced with permission.[61] Copyright 2011, Wiley-VCH. e) Optic microscope image of CNTs/PDMS-$MPU_{0.4}$-$IU_{0.6}$ electrode being cut and self-healed after 12 h from cut (top). The self-healed electrode could be further stretched to 100% strain (bottom). f) Photograph of fabricated light-emitting capacitor based on CNTs/PDMS-$MPU_{0.4}$-$IU_{0.6}$ electrode (inset). The device was stretched to 50% strain. Reproduced with permission.[10b] Copyright 2018, Nature Publishing Group.

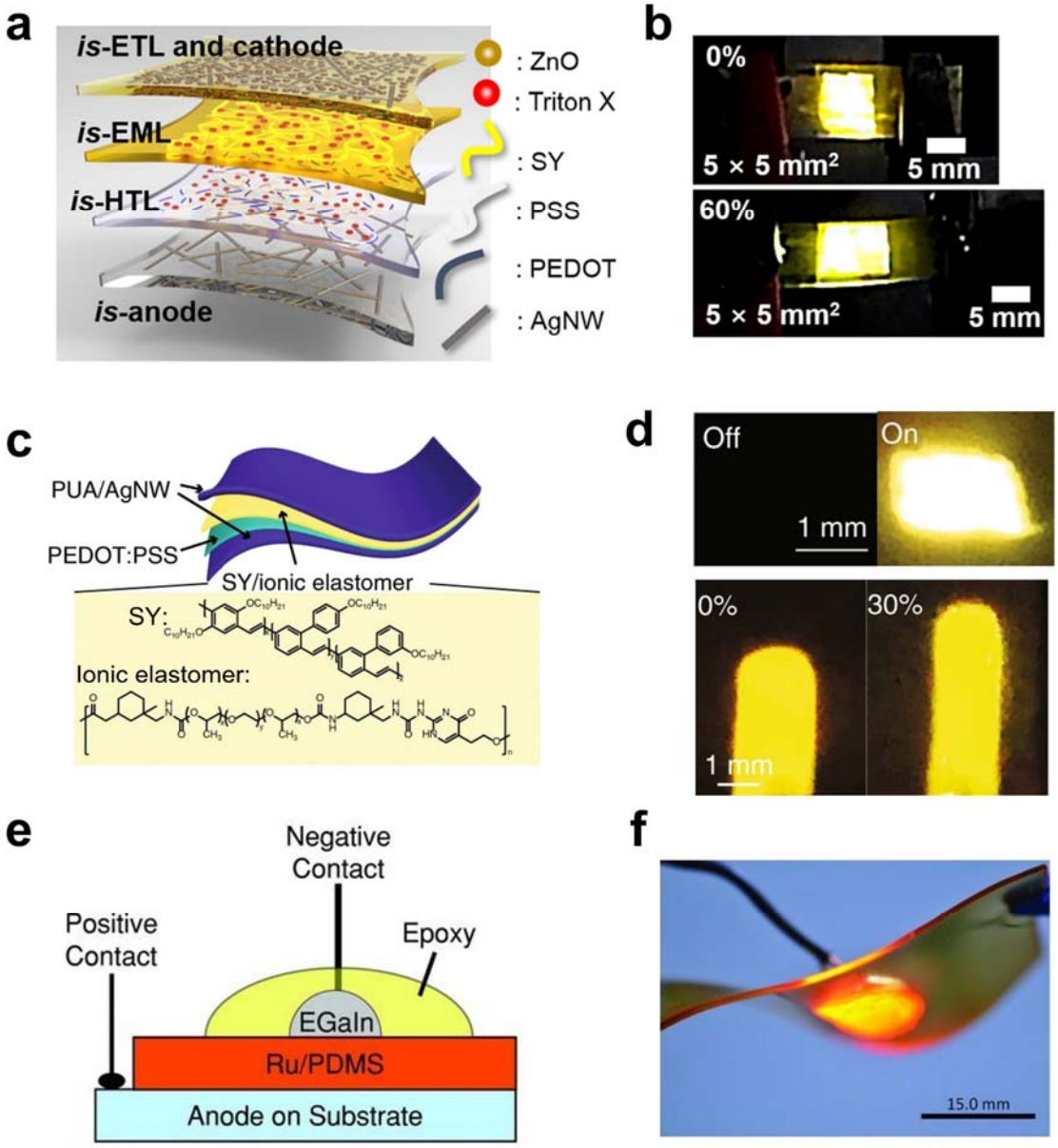

Figure 10. EL conjugated polymer with additives for intrinsically stretchable PLEDs and LECs. a) Schematic of device structure of intrinsically stretchable PLED. b) Photograph of the PELD was stretched at 0 and 60% strain. Reproduced with permission.[113] Copyright 2021, AAAS. c) Schematic of device structure of intrinsically stretchable PLEC. d) Photograph of the PELC in on and off state (top). Photograph of the PELC was stretched from 0 to 30% strain (bottom). Reproduced with permission.[119] Copyright 2020, Nature Publishing Group. e) Schematic of device structure of stretchable LEC. f) Photograph of large area LEC emitted light during stretching. Reproduced with permission.[120] Copyright 2012, Wiley-VCH.

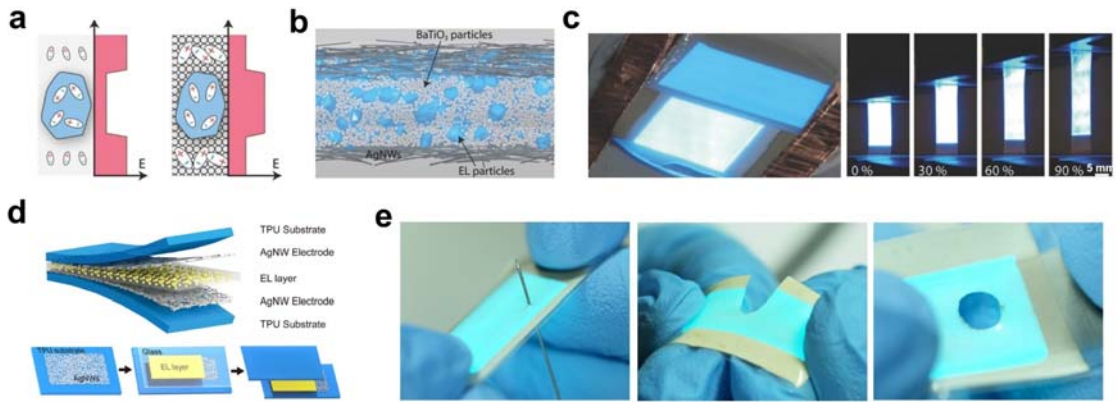

Figure 11. ZnS phosphors-composite EL layers for intrinsically stretchable ACEL devices. a) Matrix of high dielectric constant can concentrate electric field on ZnS phosphors. b) Schematic illustration of ACEL device. The EL layer was made of $BaTiO_3$, ZnS phosphors, and PDMS. c) Photograph of EL performance comparison between device without and with $BaTiO_3$ (left). Photograph of the ACEL device being stretched at 0, 30%, 60%, and 90% (right). Reproduced with permission.[23] Copyright 2016, Wiley-VCH. d) Schematic of device structure and lamination process. e) Photograph of the functional device being punctured by a needle (left), partially cut (middle), and damaged by a hole punch (right). Reproduced with permission.[129] Copyright 2018, American Chemical Society.